Cell

The Basement Membrane of Hair Follicle Stem Cells Is a Muscle Cell Niche

Hironobu Fujiwara,[1] Manuela Ferreira,[1,7] Giacomo Donati,[1] Denise K. Marciano,[2] James M. Linton,[4] Yuya Sato,[5] Andrea Hartner,[6] Kiyotoshi Sekiguchi,[5] Louis F. Reichardt,[3] and Fiona M. Watt[1,*]
[1]Cancer Research UK Cambridge Research Institute, Li Ka Shing Centre, Robinson Way, Cambridge CB2 0RE, UK
[2]Department of Medicine, Division of Nephrology
[3]Department of Physiology
University of California San Francisco, San Francisco, CA 94158, USA
[4]Fred Hutchinson Cancer Research Center, Seattle, WA 98109, USA
[5]Institute for Protein Research, Osaka University, Osaka 565-0871, Japan
[6]Department of Pediatrics and Adolescent Medicine, University of Erlangen-Nurnberg, 91054 Erlangen, Germany
[7]Present address: Immunobiology Unit, Instituto de Medicina Molecular, Faculdade de Medicina de Lisboa, 1649-028 Lisboa, Portugal
*Correspondence: fiona.watt@cancer.org.uk
DOI 10.1016/j.cell.2011.01.014

SUMMARY

The hair follicle bulge in the epidermis associates with the arrector pili muscle (APM) that is responsible for piloerection ("goosebumps"). We show that stem cells in the bulge deposit nephronectin into the underlying basement membrane, thus regulating the adhesion of mesenchymal cells expressing the nephronectin receptor, α8β1 integrin, to the bulge. Nephronectin induces α8 integrin-positive mesenchymal cells to upregulate smooth muscle markers. In nephronectin knockout mice, fewer arrector pili muscles form in the skin, and they attach to the follicle above the bulge, where there is compensatory upregulation of the nephronectin family member EGFL6. Deletion of α8 integrin also abolishes selective APM anchorage to the bulge. Nephronectin is a Wnt target; epidermal β-catenin activation upregulates epidermal nephronectin and dermal α8 integrin expression. Thus, bulge stem cells, via nephronectin expression, create a smooth muscle cell niche and act as tendon cells for the APM. Our results reveal a functional role for basement membrane heterogeneity in tissue patterning.

INTRODUCTION

The epidermis is maintained through self-renewal of stem cells and differentiation of their progeny to form the lineages of the interfollicular epidermis and adnexal structures, including the hair follicles and sebaceous glands (Watt et al., 2006). There are several distinct populations of stem cells in adult epidermis. Their properties are regulated by intrinsic transcriptional programs in response to signals from the external microenvironment, or niche (Watt and Hogan, 2000; Watt et al., 2006).

One location of epidermal stem cells is the permanent portion of the hair follicle, known as the bulge. During the resting phase of the hair growth cycle (telogen), bulge cells are in close contact with a cluster of mesenchymal cells known as the dermal papilla, and reciprocal interactions between epidermal stem cells and dermal papilla cells are essential for hair follicle formation and maintenance (Millar, 2002; Yang and Cotsarelis, 2010). A second close association between the bulge and the adjacent mesenchyme involves a smooth muscle called the arrector pili muscle (APM), which is responsible for raising the hair follicles (piloerection) to trap body heat and express emotions. Unlike the association between the bulge and the dermal papilla, which is lost during the growth (anagen) phase of the hair growth cycle, the bulge maintains contact with the APM throughout the hair cycle (Müller-Röver et al., 2001). Although it is well known that the bulge is the permanent attachment site of the APM, how attachment of the muscle is established and maintained in the bulge is entirely unknown.

We hypothesized that bulge-arrector pili muscle interactions might involve epidermal basement membrane components. Laminin-511 has been shown to mediate epidermal-dermal papilla signaling during hair development (Gao et al., 2008), and in a range of other tissues, such as kidney and pancreas, the basement membrane is involved in bidirectional cellular interactions (Linton et al., 2007; Nikolova et al., 2006). Furthermore, the basement membrane of the skin exhibits local variation in structure and composition (Timpl, 1996). Such basement membrane heterogeneity would not only provide a potential mechanism for anchoring different stem cell populations in different regions of the epidermis, but could also result in local differences in signaling with adjacent mesenchymal cells (Akiyama et al., 1995; Fuchs, 2008; Spradling et al., 2001; Watt and Hogan, 2000).

Gene expression profiling of the bulge compartment has revealed that bulge stem cells express a number of extracellular matrix (ECM) proteins that are distinct from those of other epidermal cells (Morris et al., 2004; Ohyama et al., 2006; Tumbar et al., 2004). One of these is nephronectin, an ECM protein with five EGF-like repeats, an RGD sequence, and a COOH-terminal MAM domain (Brandenberger et al., 2001). Nephronectin is an interesting candidate mediator of epidermal interactions with mesenchymal cells because the nephronectin receptor is α8β1

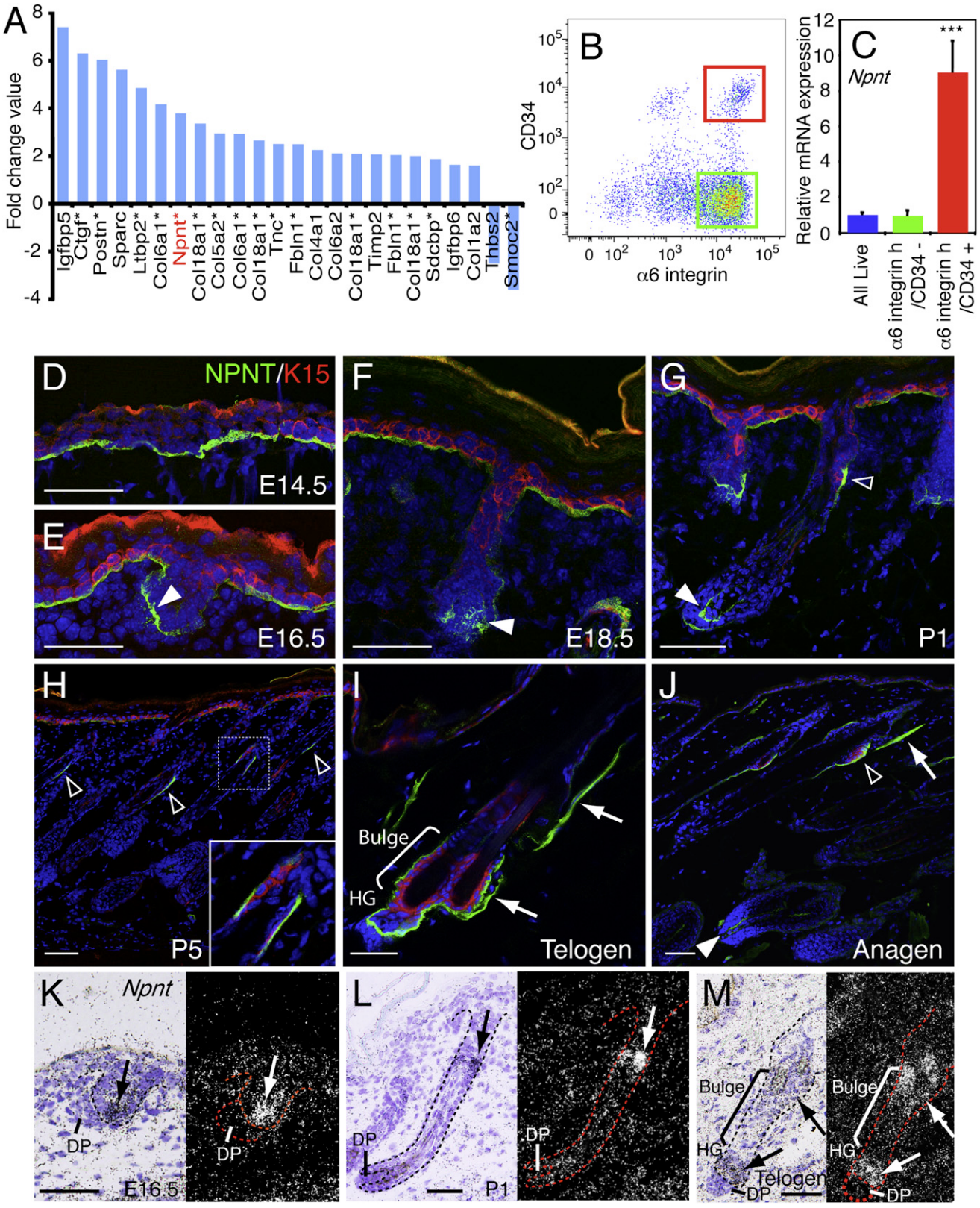
A
Fold change value
8
6
4
2
0
-2
-4
Igfbp5
Ctgf*
Postn*
Sparc
Ltbp2*
Col6a1*
Npnt*
Col18a1*
Col5a2*
Col6a1*
Col18a1*
Tnc*
Fbln1*
Col4a1
Col6a2
Col18a1*
Timp2
Fbln1*
Col18a1*
Sdcbp*
Igfbp6
Col1a2
Thbs2
Smoc2*
B
CD34
α6 integrin
C
Npnt
***
Relative mRNA expression
All Live
α6 integrin h /CD34 -
α6 integrin h /CD34 +
D
NPNT/K15
E14.5
E
E16.5
F
E18.5
G
P1
H
P5
I
Bulge
HG
Telogen
J
Anagen
K
Npnt
DP
E16.5
L
DP
P1
M
Bulge
HG
Telogen
DP

(Brandenberger et al., 2001; Sato et al., 2009), an integrin that is expressed in the dermal papilla, but not by adult epidermal keratinocytes (Driskell et al., 2009; Watt, 2002). Furthermore, the epithelial-mesenchymal interactions that are required for kidney organogenesis are disrupted in mice lacking α8β1 or nephronectin (Brandenberger et al., 2001; Linton et al., 2007; Müller et al., 1997).

In this study, we show that bulge stem cells create a specialized basement membrane containing nephronectin, which induces arrector pili muscle differentiation and anchorage to the bulge. Loss of nephronectin or α8 integrin expression causes delocalization of the APM. Thus, the bulge ECM not only contributes to the specialized niche of hair follicle stem cells, but also provides a niche for smooth muscle progenitors.

RESULTS

Bulge Stem Cells Deposit Nephronectin

By examining published microarray data, we identified a range of ECM genes that were upregulated in bulge stem cells, including nephronectin (*Npnt*) (Figure 1A and Tables S1–S3 available online). To confirm that nephronectin was upregulated in bulge cells, Q-PCR was performed on mRNA from disaggregated dorsal skin keratinocytes that had been FACS sorted on the basis of the expression of bulge stem cell markers CD34 and α6 integrin (Figure 1B). CD34+/α6 integrin^{high} cells were enriched for expression of the additional bulge maker *Sox9* and expressed low levels of *Sca1*, a marker of interfollicular epidermal cells (Figure S1A) (Jensen et al., 2009; Trempus et al., 2003). These cells had high levels of *Npnt* in comparison with unfractionated basal cells (all live; cells with low forward and side scatter) and CD34−/α6 integrin^{high} nonbulge stem cells (Figure 1C). Expression levels of other ECM genes identified from the microarrays were also confirmed by Q-PCR (Figure 1A and Figure S1A).

We next examined the distribution of nephronectin protein in embryonic and adult skin. At E14.5, nephronectin was detected throughout the epidermal-dermal basement membrane, where it was colocalized with the ubiquitous basement membrane component laminin γ1 chain (Figure 1D and Figure S1B). However, at E16.5 and E18.5, when hair follicle morphogenesis had begun, nephronectin accumulated between the hair germ and dermal condensate but was hardly detectable along the rest of the hair follicle (Figures 1E and 1F and Figure S1B). Just after birth (P1, P5), nephronectin was detected in the basement membrane of keratin 15 (K15)- and Sox9-positive early bulge stem cells as well as at the base of the follicle (Figure 1G and Figures S1B and S1C). At this time, nephronectin deposition in the bulge was asymmetrically distributed at the posterior side (Figures 1G and 1H and Figure S1B).

In adult telogen and anagen skin, nephronectin was localized to the basement membrane of the bulge, hair bulb, and APM (Figures 1I and 1J and Figure S1B). Other ECM proteins that localized to the bulge rather than along the entire outer root sheath were periostin and fibulin-1 (Figure S1D). Tenascin-C was confined to the bulge in telogen follicles but showed more widespread distribution in anagen (Figure S1D).

In situ hybridization for *Npnt* mRNA in embryonic and adult skin confirmed that nephronectin is expressed by epidermal cells. Epithelial cells of the bulge and hair germ were strongly positive for *Npnt* mRNA, whereas the dermis was negative (Figures 1K–1M). We conclude that expression of nephronectin by bulge stem cells and hair germ cells results in heterogeneity in epidermal basement membrane composition from early hair morphogenesis to adulthood.

α8 Integrin Is Specifically Expressed by Cells of the Dermal Papilla and Arrector Pili Muscle and Colocalizes with Nephronectin

Because α8β1 integrin is the major nephronectin receptor (Brandenberger et al., 2001; Sato et al., 2009), we examined whether α8β1 integrin colocalized with nephronectin in embryonic and adult skin. Whole-mount immunostaining of E14.5 dorsal skin revealed that α8 integrin was strongly expressed in dermal condensates (arrowheads in Figure 2A) and also widely expressed in the superficial dermis, correlating with the widespread distribution of nephronectin in the basement membrane (arrows in Figure 2A). Between E16.5 and E18.5, α8 integrin expression in the superficial dermis was downregulated, but it was highly expressed in the dermal condensates and dermal papillae of developing hair follicles and colocalized with nephronectin (arrowheads in Figures 2B and 2C).

At P1 and P5, α8 integrin-positive dermal cell clusters were detected in association with nephronectin in the early bulge (open arrowheads in Figures 2D and 2E) and elongated toward the interfollicular epidermis (Figure 2E), whereas α8 integrin was downregulated in dermal papillae of hair follicles in late anagen (Figures 2D and 2E). In adult telogen skin, α8 integrin accumulated at the interface between hair germ and dermal papilla, colocalizing with nephronectin (arrow in Figure 2F). The arrector pili muscles coexpressed α8 integrin and nephronectin and inserted into the nephronectin-positive bulge (Figure 2F). In addition to nephronectin, α8β1 binds to several ECM proteins,

Figure 1. Nephronectin Expression in Skin

(A) ECM genes that are upregulated or downregulated in bulge stem cells relative to other basal keratinocytes, ranked based on $\log_2$ fold change value (see Table S1). Asterisks indicate the genes that are also upregulated or downregulated in mouse label retaining cells (Tables S2 S3). Some genes are listed more than once due to their multiple spots on the array.

(B and C) Adult telogen dorsal keratinocytes were FACS sorted according to α6 integrin and CD34 expression (B). Bulge stem cells (red gate; α6 integrin^{high}/CD34+), nonbulge basal stem cells (green gate; α6 integrin^{high}/CD34−), and all live basal cells were sorted, and *Npnt* mRNA levels were determined by Q-PCR (C). Data are mean ± SEM from three mice.

(D–J) Sections of E14.5 (D), E16.5 (E), E18.5 (F), P1 (G), P5 (H), adult telogen (I), and anagen (J) skin were immunostained for nephronectin (NPNT; green) and bulge stem cell marker K15 (red), with DAPI counterstain (blue). Note nephronectin deposition in hair germ (white arrowheads), bulge (open arrowheads), and APM (arrows).

(K–M) In situ hybridization with *Npnt* probe on E16.5 (K), P1 (L), and adult telogen skin (M). Arrows indicate strong nephronectin expression. Scale bars, 50 μm. See also Figure S1 and Tables S1–S3.

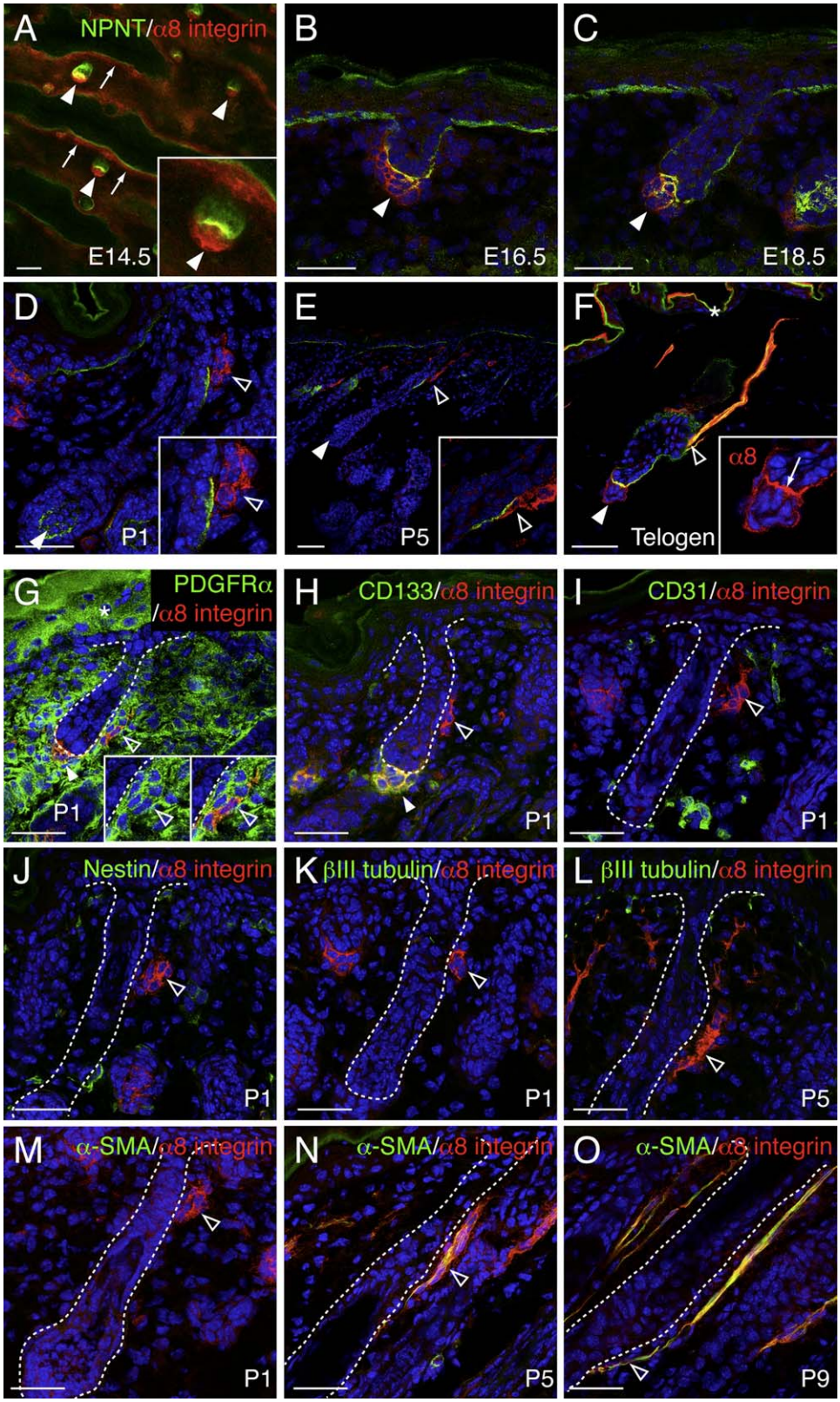
A NPNT/α8 integrin
E14.5
B
E16.5
C
E18.5
D
P1
E
P5
F
α8
Telogen
G PDGFRα /α8 integrin
P1
H CD133/α8 integrin
P1
I CD31/α8 integrin
P1
J Nestin/α8 integrin
P1
K βIII tubulin/α8 integrin
P1
L βIII tubulin/α8 integrin
P5
M α-SMA/α8 integrin
P1
N α-SMA/α8 integrin
P5
O α-SMA/α8 integrin
P9

including osteopontin, tenascin-C, fibronectin, and vitronectin (Brandenberger et al., 2001; Denda et al., 1998; Schnapp et al., 1995). However, none of these proteins showed specific colocalization with α8 integrin (Figures S2A–S2D).

To identify the α8 integrin-positive cells associated with the early bulge cells, we stained newborn skin sections with a panel of antibodies. At P1, the α8 integrin-positive population expressed dermal fibroblast markers PDGFRα and HSP47 (Figure 2G and Figure S2E) (Erez et al., 2010; Kuroda and Tajima, 2004). α8 integrin-positive cells in the dermal papilla expressed CD133 (white arrowhead in Figure 2H) (Driskell et al., 2009), but CD133 was not expressed by α8 integrin-positive cells at the bulge (open arrowhead in Figure 2H). α8 integrin-positive cells did not express the endothelial cell marker CD31, the neural crest cell derivative marker nestin, or the neuron-specific marker βIII tubulin (Figures 2I–2L). At P1, bulge-associated α8 integrin-positive cells did not express smooth muscle actin α-SMA (Figure 2M). However, from P5 onward, they were strongly positive for α-SMA (Figures 2N and 2O) and dystrophin (Figure S2F). These results suggest that the α8 integrin-positive fibroblasts associated with the bulge in P1 skin are progenitors of the APM.

α8 Integrin-Positive Dermal Cells Adhere Strongly to Nephronectin and Upregulate Smooth Muscle Markers

The specific colocalization of nephronectin and α8 integrin led us to hypothesize that nephronectin mediates adhesion of α8 integrin-positive dermal cells to the bulge basement membrane. To examine this, we performed solid-phase cell adhesion assays with purified nephronectin. Disaggregated P1 dorsal dermal cells were sorted on the basis of surface α8 integrin expression (Figure 3A). Q-PCR analysis confirmed that α8 integrin mRNA (*Itga8*) was upregulated in the α8^{high} population, whereas cells with high or low α8 integrin levels showed little variation in β1 integrin (*Itgb1*) levels (Figure 3B). Solid-phase cell adhesion assays revealed that α8 integrin^{high} dermal cells adhered strongly to nephronectin-coated substrates in a concentration-dependent manner, whereas α8 integrin^{low} dermal cells did not (Figures 3C and 3D). In contrast, both populations adhered equally well to laminin-coated substrates (Figures 3C and 3D).

Unfractionated, α8^{high} and α8^{low} cells were plated on nephronectin, laminin, or a mixture of both for 12 hr and then collected for Q-PCR analysis (Figure 3E). We examined expression of two smooth muscle cell marker genes, α-smooth muscle actin (α-SMA; *Acta2*) and smooth muscle protein 22-α (*Sm22a*), and two dermal papilla cell marker genes, *Cd133* and *Corin*. Prior to plating, α8^{high} cells expressed high levels of *Cd133* and *Corin*, consistent with their presence in dermal papillae (Figure 3E). However, expression of these markers was downregulated, regardless of whether the cells were plated on nephronectin or laminin (Figure 3E). In contrast, the α8 integrin^{high} population showed significant upregulation of *Acta2* and *Sm22a* when plated on nephronectin or nephronectin and laminin, but not on laminin alone (Figure 3E).

We conclude that nephronectin mediates adhesion of α8 integrin-positive dermal cells and stimulates expression of APM markers.

Nephronectin Is Required to Anchor Arrector Pili Muscles to the Bulge

To investigate the function of nephronectin in vivo, we analyzed *Npnt* knockout mice (Linton et al., 2007). Analysis of hematoxylin and eosin (H&E)-stained sections of adult dorsal telogen skin did not reveal any gross abnormalities, and there was no significant difference in the size of hair bulbs and dermal papillae (Figures 4A and 4B and data not shown). However, in *Npnt*$^{-/-}$ skin, α8 integrin was absent from the basement membrane separating the dermal papilla and hair germ and was more prominently distributed at the periphery of the dermal papilla (Figures S3A–S3C). The effect was specific to α8 integrin because the distribution of the phylogenetically related RGD-binding integrin subunits, αv and α5, in dermal papillae was not altered (Figures S3D and S3E). In addition, lack of nephronectin did not affect the distribution of the ubiquitous basement membrane component, laminin γ1 chain (Figure S3B).

To examine whether loss of nephronectin affected the APM, we stained sections of adult telogen dorsal skin with anti-α-SMA. In control skin, muscles were detected in association with 95.9% ± 1.2% of hair follicles. In *Npnt*$^{-/-}$ skin, there was a small but significant decrease in the percentage of hair follicles with arrector pili muscles (82.2% ± 3.3%) (Figures 4C–4E).

Given the obvious limitations of conventional histology for analyzing the spatial relationship between the APM and the hair follicle, we developed a whole-mount labeling technique in which we could observe the interaction in three dimensions. Arrector pili muscles were visualized by staining for α-SMA and SM22α, and hair follicles were visualized by DAPI labeling or Keratin 14 (K14) staining. There was an inverse gradient of α-SMA and SM22α, with α-SMA being more abundant next to the bulge and SM22α closer to the interfollicular epidermis (Figure 4F and Figure S3F). Individual muscle bundles usually branched to insert into the bulges of several neighboring hair follicles, and each follicle typically had one associated muscle bundle (Figure 4F).

Using whole-mount visualization, we confirmed the reduced number of hair follicles with associated arrector pili muscles in *Npnt*$^{-/-}$ skin: 99.7% of control follicles had an associated muscle, compared with 93.3% in knockout skin (Figures 4G–4I). There was also a significant reduction in the number of muscle attachment sites per hair follicle (Figure 4J). However,

Figure 2. Nephronectin Colocalizes with α8 Integrin-Positive Dermal Cells in Dermal Papilla and Arrector Pili Muscle

(A–F) Immunostaining for nephronectin (green) and α8 integrin (red) in developing and adult dorsal skin. (Arrows) α8 expression in superficial dermis (A) or at nephronectin-positive basement membrane between hair germ and dermal papilla (F). (White arrowheads) Dermal papilla cells. (Open arrowheads) α8 integrin-positive cells around bulge.

(G–O) Expression of α8 integrin (red) and other dermal markers (green) in postnatal dorsal skin. (Open arrowheads) α8 integrin-positive dermal cells adjacent to bulge. (White arrowhead in G and H) Dermal papilla. All sections were counterstained with DAPI (blue). Asterisk indicates nonspecific staining. Scale bars, 50 μm. See also Figure S2.

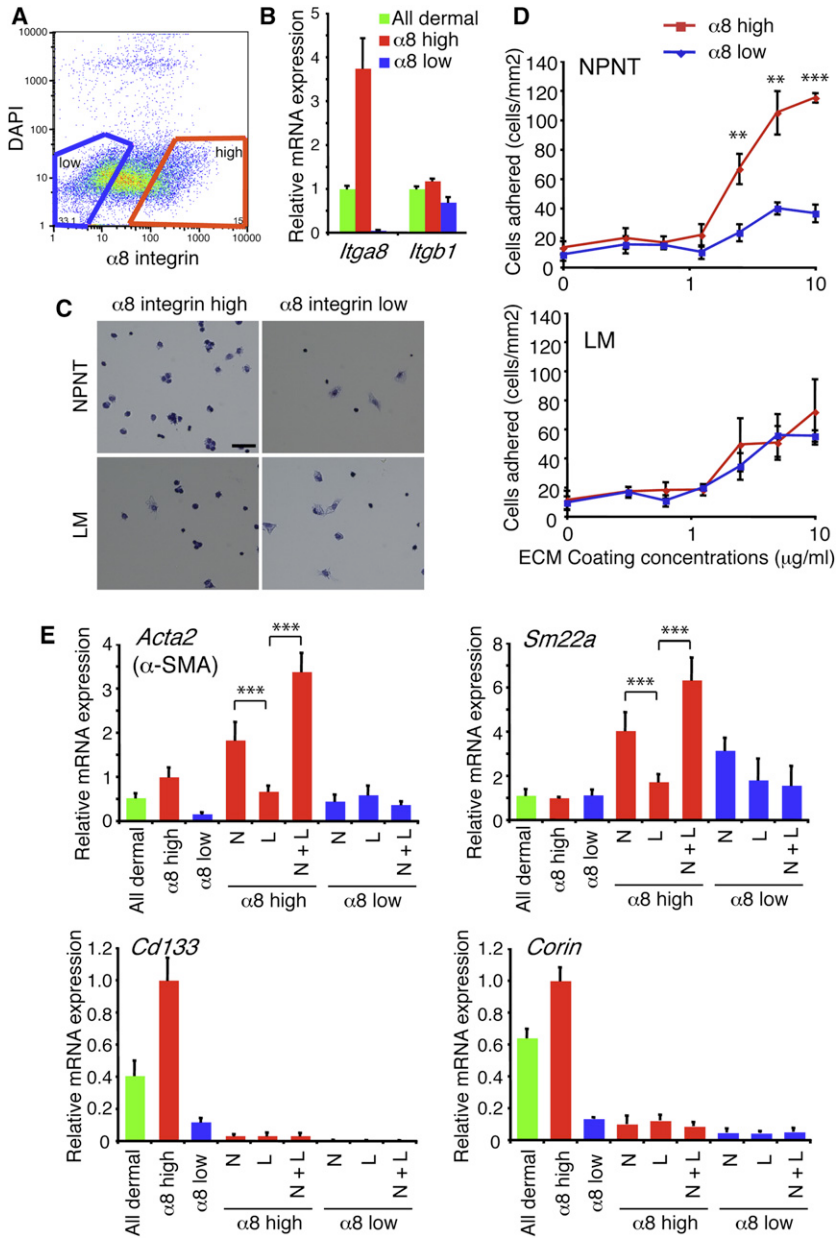

Figure 3. Adhesion and Gene Expression of Dermal Cells Plated on Nephronectin

(A and B) Disaggregated P1 dermal cells were FACS sorted on the basis of α8 integrin levels (A), and α8 integrin (*Itga8*) and β1 integrin (*Itgb1*) expression was confirmed by Q-PCR. (B). Data are means ± SEM from three mice.

(C and D) Solid-phase cell adhesion assays with FACS-sorted dermal cells plated on nephronectin (NPNT)- or laminin (LM)-coated dishes (10 μg/ml). Cells were stained with Diff Quik (C) and quantitated (D). (C) Scale bar, 50 μm. (D) Data are means ± SEM from triplicate wells.

(E) Q-PCR of smooth muscle (*Acta2* and *Sm22a*) and dermal papilla marker (*Cd133* and *Corin*) expression in unfractionated (all dermal), α8 integrin-high or integrin-low populations seeded on ECM protein-coated dishes (10 μg/ml of each protein) for 12 hr. N, nephronectin; L, laminin; N+L, nephronectin and laminin. Data are means ± SEM from three independent wells.

the major effect of *Npnt* deletion was to change the site of muscle attachment to the follicle. In control mice, the APM attached to the K15-positive bulge, whereas in *Npnt* knockout mice, the attachment was higher up the follicle (Figures 4G, 4H, and 4K–4M). In $Npnt^{+/-}$ skin, 88.3% of muscle attachments located on the bulge. However, in the knockout, only 23.2% were on the bulge, and 76.3% were located above the bulge. These results show that nephronectin is required to anchor the APM to the bulge.

The observation that loss of nephronectin led to a specific upward shift in APM insertion point, rather than randomizing the insertion sites, led us to investigate whether there was compensatory change in the distribution of the nephronectin family member EGFL6/MAEG. Like nephronectin, EGFL6 is an α8β1 ligand that is expressed in mouse skin (Osada et al., 2005). In wild-type and $Npnt^{+/-}$ skin, EGFL6 was expressed in dermal condensates at E14.5 and in the dermal sheath at E16.5–E18.5 (Figures S3G and S3H). In newborn skin (P1 and P5), EGFL6, like nephronectin, localized to the K15-positive bulge (Figure S3G and Figure 1). However, in adult skin, EGFL6 was only deposited in the basement membrane of the upper bulge, which is CD34 positive and K15 negative (Figure S3G). *Egfl6* mRNA was highly upregulated in CD34+$\alpha6^{high}$ cells relative to other basal keratinocytes (Figure S3I), indicating that EGFL6 in the upper bulge is of epidermal origin.

In control skin, the arrector pili muscles inserted below the EGFL6-positive zone of the hair follicles (Figures 4N and 4P). However, in $Npnt^{-/-}$ skin, EGFL6 deposition in the upper bulge was increased, and the muscles inserted into the EGFL6-positive zone (Figures 4O and 4P; see also Figures S3G and 3J–3L). Although the site of insertion of the APM was altered in $Npnt^{-/-}$ skin, piloerection could still be induced by treatment with the α1-adrenergic receptor agonist phenylephrine, which induces smooth muscle contraction (Figures S3M and S3N).

Our data reveal that nephronectin anchors the APM to the bulge and that, in the absence of nephronectin, the site of insertion shifts upward to the EGFL6-positive zone (Figure 4Q).

α8 Integrin Determines Specificity of Arrector Pili Muscle Attachment Site to the Bulge

Because the α8β1 integrin mediates nephronectin binding, we examined whether APM anchorage to the bulge was also disrupted in α8 integrin (*Itga8*) knockout mice (Müller et al.,

1997). H&E-stained sections of adult dorsal telogen *Itga8*$^{-/-}$ skin, like *Npnt*$^{-/-}$ skin, did not show any gross abnormalities (Figures 5A and 5B). Nephronectin deposition in the bulge was normal, but nephronectin was lacking in the APM, demonstrating that the α8 integrin is essential for deposition of nephronectin in the APM, but not in the bulge (Figures 5K and 5L). αv integrins, which, like α8, mediate nephronectin adhesion (Brandenberger et al., 2001), showed normal expression in the dermal papilla and APM of *Itga8*$^{-/-}$ skin (Figures S4A–S4D).

Arrector pili muscles were still associated with hair follicles in *Itga8*$^{-/-}$ skin, with a small reduction in the number of APM (Figures 5C and 5D and Figure S4E), but, as in the case of *Npnt*$^{-/-}$ skin, their selectivity for the bulge was disrupted. The proportion of muscles that attached to the K15-positive, nephronectin-positive, bulge region was decreased (Figures 5E–5G), and the proportion that inserted above the bulge, in the EGFL6-positive region, was increased (Figures 5H–5J). The striking difference between *Npnt*$^{-/-}$ and *Itga8*$^{-/-}$ skin was that, whereas in the absence of nephronectin, α8β1-positive APM cells showed selectivity for the EGFL6-positive region, APM lacking α8β1 lost their selectivity for nephronectin-positive basement membrane and inserted into both nephronectin- and EGFL6-positive regions (Figure 4Q and Figure 5M).

We conclude that the site of APM attachment to the hair follicle is determined by the combination of α8β1 expression on smooth muscle cells and nephronectin deposition by bulge stem cells.

Epidermal Wnt/β-Catenin Signaling Determines Regional Nephronectin and α8 Integrin Expression

Because bulge-specific expression of nephronectin creates the niche for APM cell anchorage and differentiation, we next investigated the molecular mechanism of regional nephronectin expression. The two sites of epidermal nephronectin deposition, the bulge and hair germ, are sites of active Wnt/β-catenin signaling (Lowry et al., 2005; Nguyen et al., 2009), leading us to investigate whether nephronectin is a Wnt target gene. We activated Wnt/β-catenin signaling by topical application of 4-hydroxytamoxifen (4-OHT) to the back skin of adult telogen K14ΔNβ-cateninER mice, which express stabilized β-catenin fused with the C terminus of a mutant estrogen receptor under the control of the K14 promoter (Lo Celso et al., 2004). This resulted in a 4-OHT dose-dependent increase in epidermal mRNA encoding nephronectin (Figure 6A) and the bulge Wnt effectors Tcf3 and Tcf4 (Figure S5A). In contrast, *Egfl6* mRNA levels did not change (Figure 6A). Upregulation of nephronectin protein was observed in the bulge and the ectopic hair follicles of 4-OHT-treated K14ΔNβ-cateninER mice (Figures 6B and 6C; see also Lo Celso et al., 2004), whereas deposition of EGFL6 was unaffected (Figures 6D and 6E).

Using UCSC Genome Browser, several conserved putative binding sites for Lef/Tcfs in the *Npnt* locus were identified. We therefore performed chromatin immunoprecipitation (ChIP) assays with an antibody to Tcf4, which, together with Tcf3, is specifically expressed in the bulge (Nguyen et al., 2009), and chromatin from cultured 4-OHT-treated K14ΔNβ-cateninER keratinocytes. One of the conserved sites (site 4) showed consistent enrichment for Tcf4 relative to the control FLAG antibody (Figure 6F), demonstrating that nephronectin is a direct target of Tcf4.

We then analyzed the expression of nephronectin in K14ΔNLef1 mice that express N-terminally deleted Lef1, which lacks the β-catenin-binding site, under the control of the K14 promoter (Niemann et al., 2002). ΔNLef1 acts as a dominant-negative inhibitor of Wnt/β-catenin signaling by blocking formation of β-catenin/Lef/Tcf complexes. We separated adult bulge and other basal keratinocytes from K14ΔNLef1 transgenic mice by FACS and examined the expression levels of nephronectin by Q-PCR. In bulge keratinocytes, nephronectin expression was decreased, whereas in nonbulge keratinocytes, expression was upregulated (Figure 6G). Consistent with this, in K14ΔNLef1 skin, nephronectin deposition in the bulge and hair germ was decreased, whereas nephronectin deposition in the interfollicular epidermis was increased (Figures 6H and 6I).

We also examined the effects of BMP and Notch signaling on nephronectin expression (Figures S5B and S5C). Inhibition of BMP signaling by expression of the BMP antagonist Noggin under the control of the K14 promoter (Sharov et al., 2009) increased nephronectin expression in the bulge. However, activation of Notch signaling by expression of the Notch intracellular domain via the K14 promoter (Estrach et al., 2006) did not affect nephronectin expression. The upregulation of nephronectin in K14Noggin skin fits well with the upregulation of Wnt signaling that occurs on BMP inhibition in this model (Sharov et al., 2009). These results indicate that activation of Wnt/β-catenin signaling in the bulge and hair germ induces nephronectin expression, whereas Wnt/β-catenin signaling in the interfollicular epidermis normally suppresses nephronectin.

To determine whether epidermal β-catenin activation was sufficient to induce α8β1 expression in adjacent dermal cells, we examined 4-OHT-treated mice expressing the ΔNβ-cateninER transgene. When Wnt/β-catenin signaling was activated in K14ΔNβ-cateninER transgenic mice, α8 integrin was ectopically expressed by dermal cells adjacent to ectopic hair follicles, colocalizing with nephronectin (Figures 6J–6L). When β-catenin was selectively activated in bulge stem cells by 4-OHT treatment of K15ΔNβ-cateninER mice (Baker et al., 2010), nephronectin was upregulated in the bulge and there was a corresponding increase in bulge-associated α8 integrin-expressing dermal cells (Figures 6M and 6N). These observations establish that epidermal Wnt/β-catenin signaling induces expression of α8 integrin in adjacent dermal cells.

Taken together, our data show that nephronectin is a Wnt/β-catenin target gene and that Wnt/β-catenin signaling in epidermis determines not only region-specific nephronectin deposition, but also, as a result, the location of α8 integrin-expressing mesenchymal cells.

DISCUSSION

It has previously been suggested that heterogeneity in basement membrane composition may help to establish distinct stem cell niches; however, direct evidence has been lacking (Akiyama et al., 1995; Fuchs, 2008; Hall and Watt, 1989; Scadden, 2006; Spradling et al., 2001; Watt and Hogan, 2000). Our study identifies how local variation in epidermal basement membrane composition is established and demonstrates that the specific composition of the bulge ECM not only provides a specialized

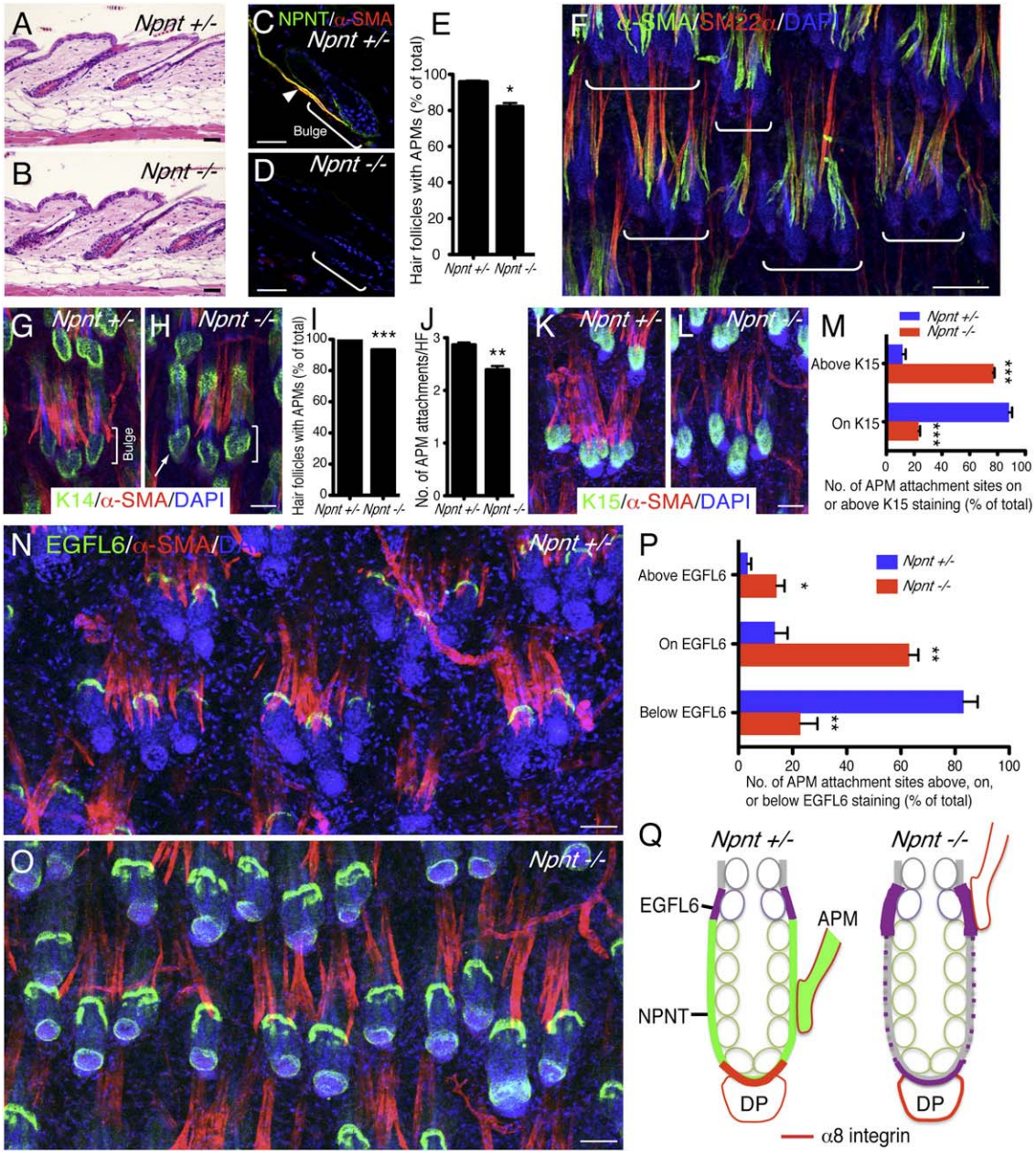

Figure 4. Nephronectin Is Required to Anchor Arrector Pili Muscles to the Bulge

(A and B) H&E-stained adult dorsal telogen skin.

(C–E) Adult dorsal skin immunostained for nephronectin (green) and α-SMA (red) and counterstained with DAPI (blue). Arrowhead indicates APM.

(E) Percentage of hair follicles with arrector pili muscles, determined from histological sections.

(F) Maximum projection image of dorsal wild-type skin whole-mount stained for α-SMA (green), SM22α (red), and nuclei (blue). White brackets indicate groups of hair follicles that share arrector pili muscles.

(G–J) Whole mounts (G and H) were immunostained for K14 (green) and α-SMA (red), with DAPI counterstain (blue). Arrow (H) indicates hair follicle without associated APM. Brackets indicate bulge. Percentage of follicles with arrector pili muscles (I) and number of APM attachments per hair follicle (J).

(K–M) Whole mounts were immunostained for K15 (green) and α-SMA (red), with DAPI counterstain (blue). Position of APM attachment sites relative to K15-positive bulge was quantified (M).

(N–P) Whole mounts were immunostained for EGFL6 (green) and α-SMA (red), with DAPI counterstain (blue). Position of APM attachment sites relative to EGFL6-positive zone was quantified (P).

(Q) Schematic summary of data. (Green) Nephronectin. (Purple) EGFL6. (Red) α8 integrin. (Green circles) K15-positive bulge cells. In the presence of nephronectin, arrector pili muscles insert at the bulge. In the absence of nephronectin, EGFL6 expression in the upper bulge is increased, and muscles insert in that region. α8 integrin colocalizes with nephronectin in the basement membrane of the hair germ adjacent to the dermal papilla (DP). In the absence of

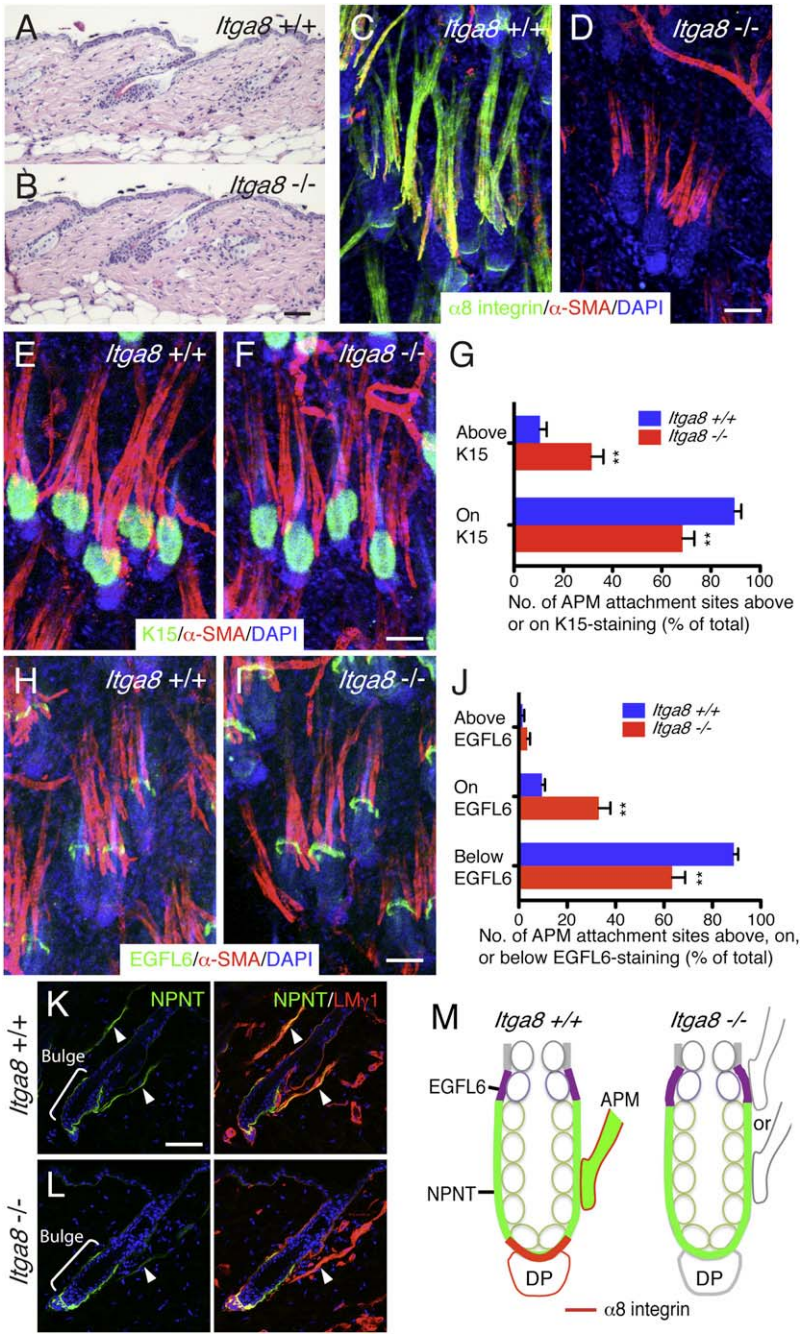

Figure 5. Deletion of α8 Integrin Disrupts Specificity of APM Attachment Site to the Bulge

(A and B) H&E-stained adult dorsal telogen skin.

(C and D) Skin whole mounts were immunostained for α8 integrin (green) and α-SMA (red), with DAPI counterstain (blue).

(E–G) Whole mounts (E and F) were immunostained for K15 (green) and α-SMA (red), with DAPI counterstain (blue). Position of APM attachment sites relative to K15-positive bulge was quantified (G).

(H–J) Whole mounts were immunostained for EGFL6 (green) and α-SMA (red), with DAPI counterstain (blue). Position of APM attachment sites relative to EGFL6-positive zone was quantified (J).

(K) Conventional cryosections were immunostained for nephronectin (green) and laminin γ1 chain (red), with DAPI counterstain (blue). Arrowheads indicate APM.

(M) Schematic summary of data. (Green) Nephronectin. (Purple) EGFL6. (Red) α8 integrin. (Green circles) K15-positive bulge cells. In the presence of α8 integrin, the APM is anchored to the bulge. In the absence of α8 integrin, muscles lose specificity for nephronectin and can anchor to both the nephronectin-positive bulge and the EGFL6-positive upper bulge regions. In the absence of α8 integrin, nephronectin deposition in the APM is disrupted, but that in the bulge is unaffected. All skin samples were from the back of 7- to 11-week-old telogen mice.

In (G) and (J), data are means ± SEM from four mice; 100 follicles per mouse. Scale bars, 50 μm. See also Figure S4.

environment for bulge stem cells, but also for adjacent mesenchymal cells (Figure 7).

Sox9-positive bulge stem cells are specified in early hair follicle morphogenesis, just after birth (Nowak et al., 2008). This coincides with restriction of nephronectin deposition to the bulge basement membrane and an associated accumulation of α8 integrin-positive mesenchymal cells, precursors of the APM. Thus, the bulge and the niche for smooth muscle progenitors are established simultaneously. Nephronectin expression is confined to the bulge basement membrane throughout adult life, irrespective of the hair cycle and consistent with the permanent association of the APM with the bulge.

We found that recombinant nephronectin not only supported adhesion of α8 integrin-positive fibroblasts from neonatal dermis, but also induced expression of smooth muscle differentiation markers, consistent with reports that α8 integrin signaling maintains differentiation of vascular smooth muscle cells (Zargham and Thibault, 2006; Zargham et al., 2007). It therefore seems likely that, during skin development, APM cells differentiate from mesenchymal progenitors through adhesion to nephronectin deposited in the early bulge. The synergistic effect of nephronectin and laminin, another component of the bulge basement membrane (Figure S1B), in inducing smooth muscle markers is consistent with the positive role of laminin in intestinal smooth muscle differentiation (Bolcato-Bellemin et al., 2003).

nephronectin, EGFL6 is expressed in that region, but there is no colocalization with α8 integrin. All skin samples were from the back of 7-week-old telogen mice.

In (E), (I), (J), (M), and (P), data are means ± SEM from three mice; 100 follicles per mouse. Scale bars, 50 μm, except for (F) (100 μm). See also Figure S3.

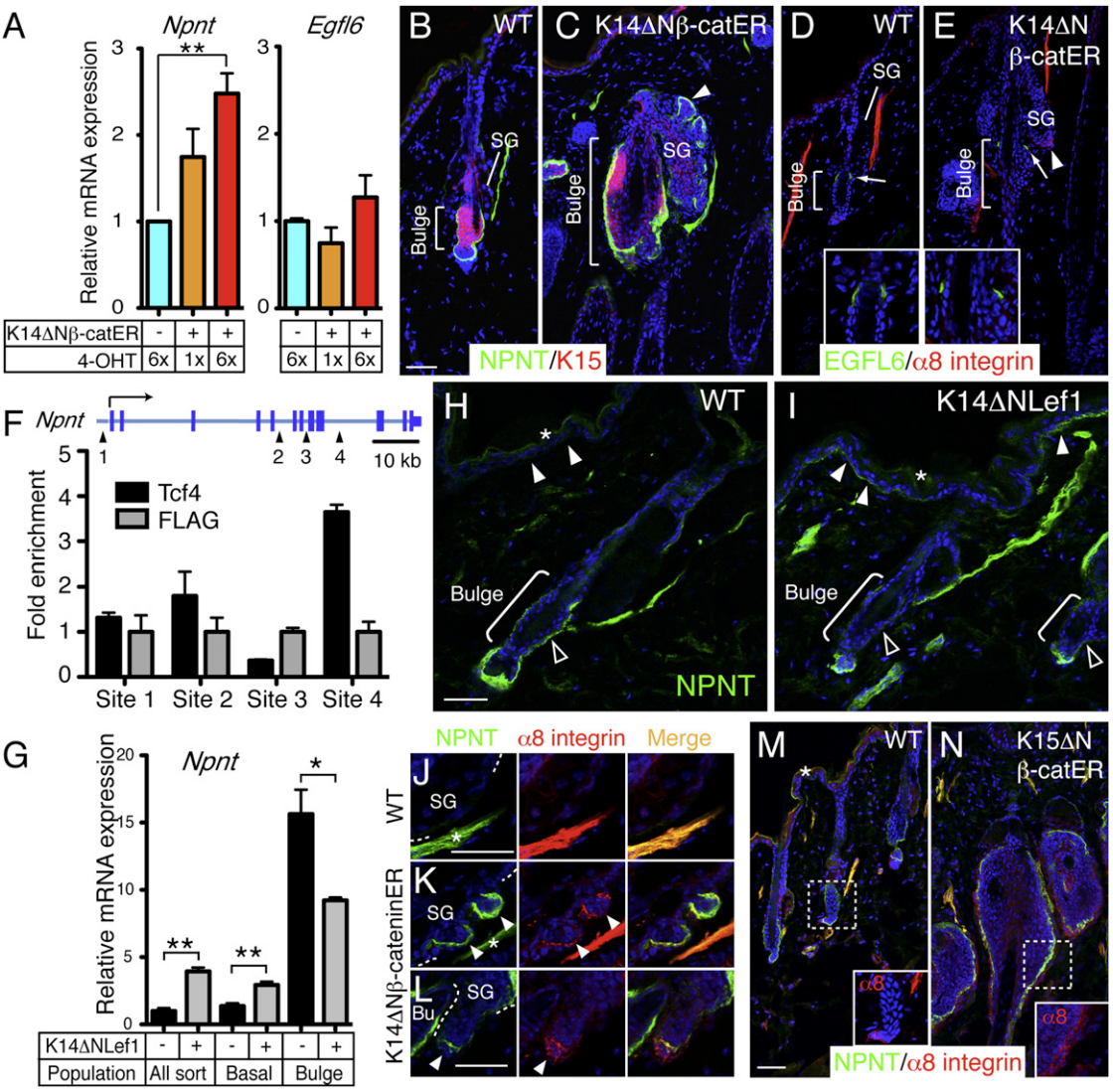

Figure 6. Regulation of Regional Nephronectin-α8 Integrin Interaction by Wnt/β-Catenin Signaling

(A) Q-PCR of *Npnt* and *Egfl6* mRNA in keratinocytes isolated from skin of wild-type (ΔNβ-catER−) and K14ΔNβ-cateninER mice (ΔNβ-catER+) that had been treated with 4-OHT for the number of times indicated. Data are means ± SEM from three mice.

(B–E) Dorsal skin of wild-type and K14ΔNβ-cateninER mice treated 6× with 4-OHT and immunostained for nephronectin (green; B and C) or EGFL6 (green; D and E) and K15 (red; B and C) or α8 integrin (red; D and E), with DAPI counterstain (blue). Arrowheads indicate ectopic hair follicle arising from sebaceous gland (SG). Arrows indicate EGFL6 staining. Inserts show higher-magnification views of EGFL6 staining around the bulge.

(F) ChIP using antibodies against Tcf4 and FLAG in K14ΔNβ-cateninER keratinocytes. Primers surrounding four conserved putative binding sites for Lef/Tcfs at the *Npnt* locus were used to detect the precipitated DNA fragments. Data are means ± SEM of two independent experiments.

(G) Q-PCR of mRNA from FACS-isolated bulge, nonbulge (basal), and total basal (all sort) keratinocytes from wild-type and K14ΔNLef1 adult telogen skin. Data are means ± SEM from three mice.

(H and I) Wild-type and K14ΔNLef1 skin immunostained for nephronectin (green), with DAPI counterstain (blue). Basement membrane of interfollicular epidermis (white arrowheads) and bulge (open arrowheads) is indicated.

(J–N) Sections of wild-type (J and M), K14ΔNβ-cateninER (K and L), and K15ΔNβ-cateninER (N) skin treated 6× (J–L) or 9× (M and N) with 4-OHT and immunostained for nephronectin (green) and α8 integrin (red), with DAPI counterstain (blue). Arrowheads indicate ectopic hair follicles. Asterisks in (J) and (K) indicate arrector pili muscles. Inserts in (M) and (N) show magnified images of α8 integrin staining around the bulge.

Asterisks in (H), (I), and (M) indicate nonspecific staining. Scale bars, 50 μm. See also Figure S5.

Deletion of nephronectin resulted in upregulation of the nephronectin-related protein EGFL6 and a corresponding change in the arrector pili muscle insertion site from the bulge to the EGFL6-positive zone above. The LFEIFEIER motif that mediates the high-affinity interaction of nephronectin with α8β1 integrin is lacking in EGFL6 (Osada et al., 2005; Sato et al., 2009), and this is the likely explanation for the specific association of α8-positive cells with nephronectin in wild-type skin. On deletion of the α8 integrin,

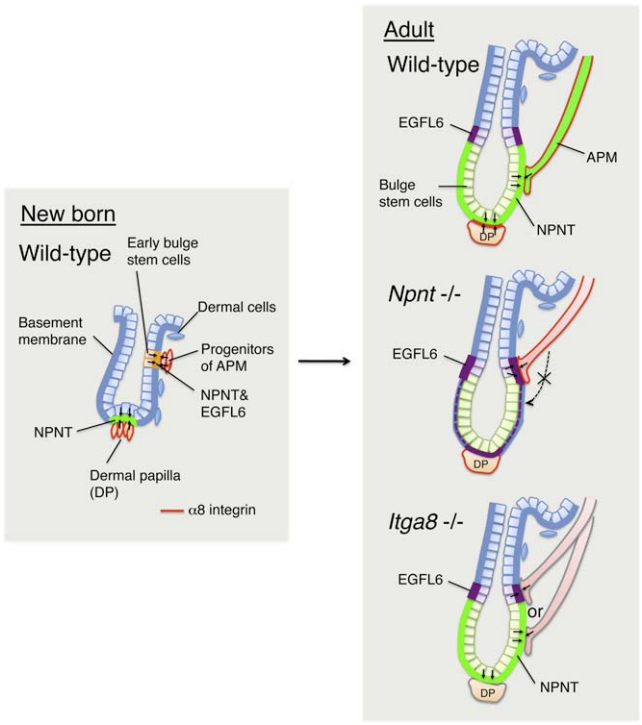

Figure 7. Model Depicting Role for Nephronectin-α8β1 Interactions in Creating the Niche for the Arrector Pili Muscle at the Hair Follicle Bulge

During hair morphogenesis in neonatal skin, early bulge stem cells locally deposit nephronectin in the bulge basement membrane. Nephronectin induces neighboring mesenchymal progenitors to differentiate into α8 integrin-positive APM cells, which adhere specifically to nephronectin, establishing a stable anchorage to the bulge that is maintained throughout adult life. In the absence of nephronectin, the APM is not anchored to the bulge but attaches above the bulge, where there is compensatory upregulation of EGFL6. Lack of nephronectin also disturbs α8 integrin-mediated hair follicle-dermal papilla interactions (Figure S3). In the absence of α8 integrin, nephronectin is still deposited in the bulge, but the selectivity of the APM interaction is lost, and muscles are anchored both to the nephronectin-positive bulge and the EGFL6-positive upper bulge.

nephronectin was still expressed in the bulge, but the specificity of APM association with nephronectin was lost, and muscles inserted into both the nephronectin-positive and EGFL6-positive zones. This is probably because, in the absence of α8β1, adhesion to nephronectin is mediated via the αv integrins, which is a lower-affinity interaction (Brandenberger et al., 2001) (Figure S4).

Though the APM is known to attach to the bulge via a tendon, the tendon cells have not been identified (Barcaui et al., 2002; Guerra Rodrigo et al., 1975). We showed that the tendon/ligament extracellular matrix protein periostin (Horiuchi et al., 1999; Norris et al., 2007) was strongly expressed in bulge stem cells and deposited locally around the bulge. Furthermore, the gene signature of bulge stem cells includes many tendon-related genes, such as *Scx* (scleraxis), *Mitf*, *Igfbp5*, *Fbln1* (fibulin-1), *Postn* (periostin), *Tnc* (tenascin-C), *Sparc*, *Igfbp6*, and *Fgf18* (Brent et al., 2003; Jelinsky et al., 2010; Morris et al., 2004; Tumbar et al., 2004). We therefore propose that bulge stem cells function as tendon cells in providing a physical connection for the APM. The immobility of the bulge ensures that APM attachment is stable regardless of the stage of the hair growth cycle.

We did not obtain any evidence that, as has been suggested, the APM determines the location of bulge stem cells (Akiyama et al., 1995; Christiano, 2004). The delocalization of the muscle that occurred on loss of nephronectin had no clear effect on the bulge, as judged by bulge morphology and expression of keratin 15 and CD34. Thus, nephronectin expression by bulge stem cells provides a niche for APM cells but is not an essential component of the epidermal stem cell niche.

Wnt/β-catenin signaling is well known to play a role in controlling epidermal stem cell renewal and lineage selection and in reciprocal interactions with the dermal papilla (Alonso and Fuchs, 2003; Watt and Collins, 2008). However, a role for Wnt/β-catenin signaling in regulating the APM was previously unknown. We demonstrate that nephronectin, unlike EGFL6, is a direct target of Wnt/β-catenin signaling. Nephronectin expression is upregulated by Wnt/β-catenin activation, directly or via inhibition of BMP signaling, in the epidermis, and as a result, there is a corresponding upregulation of α8 integrin expression in the adjacent dermis.

The consequences of activating Wnt/β-catenin signaling were context dependent. Activation in the bulge upregulated nephronectin, whereas activation in the interfollicular epidermis did not. Conversely, expression of ΔNLef1, which inhibits Wnt signaling, stimulated nephronectin expression in the interfollicular epidermis and downregulated expression in the bulge. A likely explanation for the region-specific effects of ΔNLef1 is that ΔNLef1 expression in the bulge inhibits β-catenin-dependent induction of nephronectin expression by Tcf3 or Tcf4, whereas in the interfollicular epidermis, Tcf/Lef transcription factors are not expressed, so ΔNLef1 regulates nephronectin expression independently of the Wnt pathway (Nguyen et al., 2006).

The APM plays an important role in thermoregulation because it is responsible for piloerection, which traps warm air at the skin surface. Piloerection is also believed to cause constriction of the sebaceous glands, aiding release of sebum onto the skin surface (Poblet et al., 2004). Furthermore, as Charles Darwin noted in 1872, involuntary erection of hairs, feathers, and other dermal appendages is an evolutionarily conserved response to emotional disturbance (Darwin, 1872). Our results provide new insights into the mechanism of arrector pili muscle morphogenesis and answer the long-standing question of why the arrector pili muscle is attached to the hair follicle bulge (Akiyama et al., 1995).

EXPERIMENTAL PROCEDURES

Generation and Experimental Treatment of Mice

Npnt knockout mice, *Itga8* knockout mice, and K14ΔNLef1, K14ΔNβ-cateninER (D2 line), and K15ΔNβ-cateninER transgenic mice have been described previously (Baker et al., 2010; Linton et al., 2007; Lo Celso et al., 2004; Müller et al., 1997; Niemann et al., 2002). The ΔNβ-cateninER transgene was activated by topical application of 4-hydroxytamoxifen (4-OHT; Sigma) dissolved in acetone. Shaved back skin was treated topically with 1.5 mg of 4-OHT in 200 μl of acetone three times per week for 2 weeks unless otherwise specified.

Gene Expression Analysis

For microarray analysis, CEL format files of the gene expression profiles of K15-positive mouse bulge stem cells (GSE1096) were obtained from the NCBI's GEO (Gene Expression Omnibus) website (Morris et al., 2004) and were analyzed with Genespring X10.0 (Agilent Technologies).

Immunohistochemistry and Whole-Mount Preparations

Immunofluorescence staining of tissue sections was performed by conventional methods. Whole-mount immunostaining of mouse dorsal skin was performed by applying the methods established for whole-mount immunostaining of mouse tail epidermis, with some modifications (Braun et al., 2003). Embryonic and adult dorsal skin was dissected, and the subcutaneous fat tissue was removed. Skin was fixed with 4% paraformaldehyde/PBS for 1 hr at room temperature and blocked with a blocking buffer for 1 hr. Skin samples were incubated with primary antibodies diluted in blocking buffer overnight at room temperature, washed with 0.2% Tween 20/PBS for 4 hr, and then incubated with DAPI and secondary antibodies diluted in blocking buffer overnight at room temperature. Finally, skin samples were washed with 0.2% Tween 20/PBS for 4 hr at room temperature and mounted.

Images were acquired using a Leica TCS SP5 Tandem Scanner confocal microscope. Z stack maximum projection images of whole-mount preparations were produced using LAS AF software (Leica).

Quantitative RT-PCR

Total RNA was isolated using an RNeasy Mini kit (QIAGEN) with on-column DNase I digestion. cDNA was synthesized using SuperScript III (Invitrogen). RT-PCR was performed using SYBR green super mix (ABI). The expression levels of target genes were normalized by *Gapdh* levels utilizing a standard curve method. Primers used in this study are listed in Supplemental Information.

FACS

Mouse adult dorsal telogen keratinocytes were isolated, stained for α6 integrin and CD34, and sorted as described previously (Silva-Vargas et al., 2005). For dermal cell sorting, P1 newborn dorsal skin was treated with 5 mM EDTA/PBS at 37°C for 3 hr. The epidermal sheet, including hair follicles, was peeled off and discarded. The dermis was incubated in FAD medium containing 0.2% collagenase (GIBCO) and 2U/ml of DNase I (Sigma) at 37°C for 1 hr. The dermal cell suspension was stained for α8 integrin. Cells were sorted with a FACSAria according to α8 integrin expression after gating out dead cells and cells with high forward and side scatter.

Statistics

P values were determined using the Student's t test: *P < 0.05; **p < 0.01; ***p < than 0.001.

Additional Experimental Procedures

These are described in the Supplemental Information.

SUPPLEMENTAL INFORMATION

Supplemental Information includes Extended Experimental Procedures, five figures, and five tables and can be found with this article online at doi:10.1016/j.cell.2011.01.014.

ACKNOWLEDGMENTS

We thank Vladimir Botchkarev for K14-Noggin skin and Takako Sasaki for Fibulin-1 antibody. We gratefully acknowledge the technical assistance of the core resources of the CRUK Cambridge Research Institute. We thank the entire Watt lab for valuable reagents, suggestions, and advice. This work was funded by Cancer Research UK and supported by the University of Cambridge and Hutchison Whampoa Ltd. We also gratefully acknowledge financial support from the NIH (NS19090 to L.F.R.), from the Uehara Memorial Foundation (H.F.), and from EU FP7 (Optistem).

Received: July 2, 2010
Revised: October 24, 2010
Accepted: January 10, 2011
Published: February 17, 2011

REFERENCES

Akiyama, M., Dale, B.A., Sun, T.T., and Holbrook, K.A. (1995). Characterization of hair follicle bulge in human fetal skin: the human fetal bulge is a pool of undifferentiated keratinocytes. J. Invest. Dermatol. *105*, 844–850.

Alonso, L., and Fuchs, E. (2003). Stem cells in the skin: waste not, Wnt not. Genes Dev. *17*, 1189–1200.

Baker, C.M., Verstuyf, A., Jensen, K.B., and Watt, F.M. (2010). Differential sensitivity of epidermal cell subpopulations to beta-catenin-induced ectopic hair follicle formation. Dev. Biol. *343*, 40–50.

Barcaui, C.B., Piñeiro-Maceira, J., and de Avelar Alchorne, M.M. (2002). Arrector pili muscle: evidence of proximal attachment variant in terminal follicles of the scalp. Br. J. Dermatol. *146*, 657–658.

Bolcato-Bellemin, A.L., Lefebvre, O., Arnold, C., Sorokin, L., Miner, J.H., Kedinger, M., and Simon-Assmann, P. (2003). Laminin alpha5 chain is required for intestinal smooth muscle development. Dev. Biol. *260*, 376–390.

Brandenberger, R., Schmidt, A., Linton, J., Wang, D., Backus, C., Denda, S., Müller, U., and Reichardt, L.F. (2001). Identification and characterization of a novel extracellular matrix protein nephronectin that is associated with integrin alpha8beta1 in the embryonic kidney. J. Cell Biol. *154*, 447–458.

Braun, K.M., Niemann, C., Jensen, U.B., Sundberg, J.P., Silva-Vargas, V., and Watt, F.M. (2003). Manipulation of stem cell proliferation and lineage commitment: visualisation of label-retaining cells in wholemounts of mouse epidermis. Development *130*, 5241–5255.

Brent, A.E., Schweitzer, R., and Tabin, C.J. (2003). A somitic compartment of tendon progenitors. Cell *113*, 235–248.

Christiano, A.M. (2004). Epithelial stem cells: stepping out of their niche. Cell *118*, 530–532.

Darwin, C. (1872). The expression of the emotions in man and animals (London: J. Murray).

Denda, S., Reichardt, L.F., and Müller, U. (1998). Identification of osteopontin as a novel ligand for the integrin alpha8 beta1 and potential roles for this integrin-ligand interaction in kidney morphogenesis. Mol. Biol. Cell *9*, 1425–1435.

Driskell, R.R., Giangreco, A., Jensen, K.B., Mulder, K.W., and Watt, F.M. (2009). Sox2-positive dermal papilla cells specify hair follicle type in mammalian epidermis. Development *136*, 2815–2823.

Erez, N., Truitt, M., Olson, P., Arron, S.T., and Hanahan, D. (2010). Cancer-associated fibroblasts are activated in incipient neoplasia to orchestrate tumor-promoting inflammation in an NF-kappaB-dependent manner. Cancer Cell *17*, 135–147.

Estrach, S., Ambler, C.A., Lo Celso, C., Hozumi, K., and Watt, F.M. (2006). Jagged 1 is a beta-catenin target gene required for ectopic hair follicle formation in adult epidermis. Development *133*, 4427–4438.

Fuchs, E. (2008). Skin stem cells: rising to the surface. J. Cell Biol. *180*, 273–284.

Gao, J., DeRouen, M.C., Chen, C.H., Nguyen, M., Nguyen, N.T., Ido, H., Harada, K., Sekiguchi, K., Morgan, B.A., Miner, J.H., et al. (2008). Laminin-511 is an epithelial message promoting dermal papilla development and function during early hair morphogenesis. Genes Dev. *22*, 2111–2124.

Guerra Rodrigo, F., Cotta-Pereira, G., and David-Ferreira, J.F. (1975). The fine structure of the elastic tendons in the human arrector pili muscle. Br. J. Dermatol. *93*, 631–637.

Hall, P.A., and Watt, F.M. (1989). Stem cells: the generation and maintenance of cellular diversity. Development *106*, 619–633.

Horiuchi, K., Amizuka, N., Takeshita, S., Takamatsu, H., Katsuura, M., Ozawa, H., Toyama, Y., Bonewald, L.F., and Kudo, A. (1999). Identification and characterization of a novel protein, periostin, with restricted expression to periosteum and periodontal ligament and increased expression by transforming growth factor beta. J. Bone Miner. Res. *14*, 1239–1249.

Jelinsky, S.A., Archambault, J., Li, L., and Seeherman, H. (2010). Tendon-selective genes identified from rat and human musculoskeletal tissues. J. Orthop. Res. *28*, 289–297.

Jensen, K.B., Collins, C.A., Nascimento, E., Tan, D.W., Frye, M., Itami, S., and Watt, F.M. (2009). Lrig1 expression defines a distinct multipotent stem cell population in mammalian epidermis. Cell Stem Cell *4*, 427–439.

Kuroda, K., and Tajima, S. (2004). HSP47 is a useful marker for skin fibroblasts in formalin-fixed, paraffin-embedded tissue specimens. J. Cutan. Pathol. *31*, 241–246.

Linton, J.M., Martin, G.R., and Reichardt, L.F. (2007). The ECM protein nephronectin promotes kidney development via integrin alpha8beta1-mediated stimulation of Gdnf expression. Development *134*, 2501–2509.

Lo Celso, C., Prowse, D.M., and Watt, F.M. (2004). Transient activation of beta-catenin signalling in adult mouse epidermis is sufficient to induce new hair follicles but continuous activation is required to maintain hair follicle tumours. Development *131*, 1787–1799.

Lowry, W.E., Blanpain, C., Nowak, J.A., Guasch, G., Lewis, L., and Fuchs, E. (2005). Defining the impact of beta-catenin/Tcf transactivation on epithelial stem cells. Genes Dev. *19*, 1596–1611.

Millar, S.E. (2002). Molecular mechanisms regulating hair follicle development. J. Invest. Dermatol. *118*, 216–225.

Morris, R.J., Liu, Y., Marles, L., Yang, Z., Trempus, C., Li, S., Lin, J.S., Sawicki, J.A., and Cotsarelis, G. (2004). Capturing and profiling adult hair follicle stem cells. Nat. Biotechnol. *22*, 411–417.

Müller, U., Wang, D., Denda, S., Meneses, J.J., Pedersen, R.A., and Reichardt, L.F. (1997). Integrin alpha8beta1 is critically important for epithelial-mesenchymal interactions during kidney morphogenesis. Cell *88*, 603–613.

Müller-Röver, S., Handjiski, B., van der Veen, C., Eichmüller, S., Foitzik, K., McKay, I.A., Stenn, K.S., and Paus, R. (2001). A comprehensive guide for the accurate classification of murine hair follicles in distinct hair cycle stages. J. Invest. Dermatol. *117*, 3–15.

Nguyen, H., Rendl, M., and Fuchs, E. (2006). Tcf3 governs stem cell features and represses cell fate determination in skin. Cell *127*, 171–183.

Nguyen, H., Merrill, B.J., Polak, L., Nikolova, M., Rendl, M., Shaver, T.M., Pasolli, H.A., and Fuchs, E. (2009). Tcf3 and Tcf4 are essential for long-term homeostasis of skin epithelia. Nat. Genet. *41*, 1068–1075.

Niemann, C., Owens, D.M., Hülsken, J., Birchmeier, W., and Watt, F.M. (2002). Expression of DeltaNLef1 in mouse epidermis results in differentiation of hair follicles into squamous epidermal cysts and formation of skin tumours. Development *129*, 95–109.

Nikolova, G., Jabs, N., Konstantinova, I., Domogatskaya, A., Tryggvason, K., Sorokin, L., Fässler, R., Gu, G., Gerber, H.P., Ferrara, N., et al. (2006). The vascular basement membrane: a niche for insulin gene expression and Beta cell proliferation. Dev. Cell *10*, 397–405.

Norris, R.A., Damon, B., Mironov, V., Kasyanov, V., Ramamurthi, A., Moreno-Rodriguez, R., Trusk, T., Potts, J.D., Goodwin, R.L., Davis, J., et al. (2007). Periostin regulates collagen fibrillogenesis and the biomechanical properties of connective tissues. J. Cell. Biochem. *101*, 695–711.

Nowak, J.A., Polak, L., Pasolli, H.A., and Fuchs, E. (2008). Hair follicle stem cells are specified and function in early skin morphogenesis. Cell Stem Cell *3*, 33–43.

Ohyama, M., Terunuma, A., Tock, C.L., Radonovich, M.F., Pise-Masison, C.A., Hopping, S.B., Brady, J.N., Udey, M.C., and Vogel, J.C. (2006). Characterization and isolation of stem cell-enriched human hair follicle bulge cells. J. Clin. Invest. *116*, 249–260.

Osada, A., Kiyozumi, D., Tsutsui, K., Ono, Y., Weber, C.N., Sugimoto, N., Imai, T., Okada, A., and Sekiguchi, K. (2005). Expression of MAEG, a novel basement membrane protein, in mouse hair follicle morphogenesis. Exp. Cell Res. *303*, 148–159.

Poblet, E., Jiménez, F., and Ortega, F. (2004). The contribution of the arrector pili muscle and sebaceous glands to the follicular unit structure. J. Am. Acad. Dermatol. *51*, 217–222.

Sato, Y., Uemura, T., Morimitsu, K., Sato-Nishiuchi, R., Manabe, R., Takagi, J., Yamada, M., and Sekiguchi, K. (2009). Molecular basis of the recognition of nephronectin by integrin alpha8beta1. J. Biol. Chem. *284*, 14524–14536.

Scadden, D.T. (2006). The stem-cell niche as an entity of action. Nature *441*, 1075–1079.

Schnapp, L.M., Hatch, N., Ramos, D.M., Klimanskaya, I.V., Sheppard, D., and Pytela, R. (1995). The human integrin alpha 8 beta 1 functions as a receptor for tenascin, fibronectin, and vitronectin. J. Biol. Chem. *270*, 23196–23202.

Sharov, A.A., Mardaryev, A.N., Sharova, T.Y., Grachtchouk, M., Atoyan, R., Byers, H.R., Seykora, J.T., Overbeek, P., Dlugosz, A., and Botchkarev, V.A. (2009). Bone morphogenetic protein antagonist noggin promotes skin tumorigenesis via stimulation of the Wnt and Shh signaling pathways. Am. J. Pathol. *175*, 1303–1314.

Silva-Vargas, V., Lo Celso, C., Giangreco, A., Ofstad, T., Prowse, D.M., Braun, K.M., and Watt, F.M. (2005). Beta-catenin and Hedgehog signal strength can specify number and location of hair follicles in adult epidermis without recruitment of bulge stem cells. Dev. Cell *9*, 121–131.

Spradling, A., Drummond-Barbosa, D., and Kai, T. (2001). Stem cells find their niche. Nature *414*, 98–104.

Timpl, R. (1996). Macromolecular organization of basement membranes. Curr. Opin. Cell Biol. *8*, 618–624.

Trempus, C.S., Morris, R.J., Bortner, C.D., Cotsarelis, G., Faircloth, R.S., Reece, J.M., and Tennant, R.W. (2003). Enrichment for living murine keratinocytes from the hair follicle bulge with the cell surface marker CD34. J. Invest. Dermatol. *120*, 501–511.

Tumbar, T., Guasch, G., Greco, V., Blanpain, C., Lowry, W.E., Rendl, M., and Fuchs, E. (2004). Defining the epithelial stem cell niche in skin. Science *303*, 359–363.

Watt, F.M. (2002). Role of integrins in regulating epidermal adhesion, growth and differentiation. EMBO J. *21*, 3919–3926.

Watt, F.M., and Hogan, B.L. (2000). Out of Eden: stem cells and their niches. Science *287*, 1427–1430.

Watt, F.M., and Collins, C.A. (2008). Role of beta-catenin in epidermal stem cell expansion, lineage selection, and cancer. Cold Spring Harb. Symp. Quant. Biol. *73*, 503–512.

Watt, F.M., Lo Celso, C., and Silva-Vargas, V. (2006). Epidermal stem cells: an update. Curr. Opin. Genet. Dev. *16*, 518–524.

Yang, C.C., and Cotsarelis, G. (2010). Review of hair follicle dermal cells. J. Dermatol. Sci. *57*, 2–11.

Zargham, R., and Thibault, G. (2006). Alpha 8 integrin expression is required for maintenance of the smooth muscle cell differentiated phenotype. Cardiovasc. Res. *71*, 170–178.

Zargham, R., Touyz, R.M., and Thibault, G. (2007). alpha 8 Integrin overexpression in de-differentiated vascular smooth muscle cells attenuates migratory activity and restores the characteristics of the differentiated phenotype. Atherosclerosis *195*, 303–312.

Cell

EXTENDED EXPERIMENTAL PROCEDURES

Gene Expression Analysis

For microarray analysis, CEL format files of the gene expression profiles of keratin 15-positive mouse bulge stem cells (GSE1096) were obtained from the NCBI's GEO (Gene Expression Omnibus) website (Morris et al., 2004) and analyzed with Genespring X10.0 (Agilent Technologies). After RMA normalization, un-paired t test and fold-change analysis were performed and ECM genes that showed p-values < 0.05 and fold change values > 1.5 (log2 fold change) were selected. In addition, DAT format files of the gene expression profiles of mouse skin label-retaining cells were obtained from the Fuchs Lab web site (Tumbar et al., 2004), converted to CEL format files and analyzed using R version 2.7.1 and various bioconductor packages, including *affy* and *limma*. Two pairwise comparisons between arrays, "GFP high and GFP low" and "GFP high and beta4," were carried out. ECM genes that showed an adjusted p-value of < 0.05 and fold change value of > 1.5 (log2 fold change) were selected.

Quantitative RT-PCR

Total RNA was isolated using an RNeasy Mini kit (QIAGEN) with on-column DNase I digestion. cDNA was synthesized using SuperScript III (Invitrogen). RT-PCR was performed on an ABI7900HT using SYBR green super mix (ABI). The expression levels of target genes were normalized by *Gapdh* levels utilizing a standard curve method. Primers used in this study are listed in Table S4.

For quantitative RT-PCR of K14ΔNβ-cateninER transgenic epidermis, subcutaneous fat was removed from dissected dorsal skin and the remaining skin was incubated with 2U/ml of Dispase (GIBCO) in FAD medium overnight at 4°C. Epidermis, including hair follicles, was separated from dermis by gentle scraping with a scalpel. Total epidermal RNA was isolated as described above.

Immunohistochemistry and Whole-Mount Preparations

Immunofluorescence staining was performed on frozen sections that had been fixed with 4% paraformaldehyde/PBS for 2 min and then blocked with 10% FBS/0.1% Triton X-100/PBS for 30 min at room temperature. Sections were incubated with primary antibodies diluted in blocking buffer at 4°C overnight. Secondary antibodies (Alexa-488- and −555-conjugated) were diluted in blocking buffer and applied to sections for 1 hr at room temperature together with DAPI to label nuclei.

Whole-mount immunostaining of mouse dorsal skin was performed by applying the methods established for whole-mount immunostaining of mouse tail epidermis, with some modifications (Braun et al., 2003). Embryonic and adult dorsal skin was dissected and the subcutaneous fat tissue was removed with a scalpel. Skin was fixed with 4% paraformaldehyde/PBS for 1 hr at room temperature and blocked with 20 mM HEPES buffer (pH 7.2) containing 0.5% skim milk powder, 0.25% fish skin gelatin (Sigma), 0.5% Triton X-100, and 0.9% NaCl for 1 hr at room temperature. Skin samples were incubated with primary antibodies diluted in blocking buffer overnight at room temperature, washed with 0.2% Tween 20/PBS for 4 hr and then incubated with DAPI and secondary antibodies (Alexa-555- and −633-conjugated) diluted in blocking buffer overnight at room temperature. Skin samples were washed with 0.2% Tween 20/PBS for 4 hr at room temperature and mounted. Mounted samples were stored at 4°C for at least 2 days before analysis in order to increase the transparency of the samples.

Images were acquired using a Leica TCS SP5 Tandem Scanner confocal microscope. Z-stack maximum projection images of whole-mount preparations were produced using LAS AF software (Leica).

Antibodies

Rabbit antiserum to nephronectin was generated by immunizing rabbits with FLAG-tagged mouse nephronectin (Sato et al., 2009). The antibody was affinity-purified with 6xHis-tagged mouse nephronectin coupled to CNBr-activated Sepharose 4B. Rabbit anti-mouse EGFL6/MAEG was generated as described previously (Osada et al., 2005). Mouse anti-keratin 15 (LHK15) and mouse anti-keratin 14 (LL002) antibodies were provided in-house by Cancer Research UK Research Services. Goat anti-mouse α8 integrin (R&D), rat anti-mouse PDGFRα (BioLegend), rat anti-mouse CD133 (eBioscience), rat anti-mouse CD31 (BD), mouse anti-rat nestin (Chemicon), mouse anti-rat βIII tubulin (abcam), mouse anti-α-SMA (Sigma), rat anti-mouse laminin γ1 (Chemicon), rabbit anti-mouse SM22α (abcam), CD34-Alexa647 (eBioscience) and α6 integrin-FITC (BD) were purchased from the companies indicated. More information about the antibodies is provided in Table S5.

FACS

Mouse adult dorsal telogen keratinocytes were isolated and stained for α6 integrin and CD34 as described previously (Silva-Vargas et al., 2005). Cell viability was assessed by DAPI-staining. Cells were sorted with a FACSAria according to α6 integrin and CD34 expression, after gating out dead cells and cells with high forward and side scatter.

For dermal cell sorting, P1 newborn dorsal skin was treated with 5 mM EDTA/PBS at 37°C for 3 hr. The epidermal sheet, including hair follicles, was peeled off and discarded. The dermis was incubated for 10 min in FAD medium, minced with a scalpel, then incubated in FAD medium containing 0.2% collagenase (GIBCO) and 2U/ml of DNase I (Sigma) at 37°C for 1 hr with gentle inversion. The cell suspension was filtered with a 40 μm mesh strainer to remove muscle fragments, blood vessels and contaminating hair follicles. The dermal cell suspension was stained for α8 integrin, and cell viability was assessed by DAPI-staining. Cells were sorted with a FACSAria according to α8 integrin expression, after gating out dead cells and cells with high forward and side scatter.

Solid-Phase Cell Adhesion Assay

Solid-phase cell adhesion assays were performed as described previously (Fujiwara et al., 2001) with minor modifications. Briefly, FLAG-tagged mouse full-length nephronectin was purified as described previously (Sato et al., 2009). Ninety six-well cell culture plates were coated with nephronectin and human laminin (Chemicon) and blocked with 1% heat-denatured bovine serum albumin. FACS sorted-dermal cells were suspended in serum-free DMEM, plated on the coated plates, and incubated for 2 hr in a CO_2 incubator at 37°C. Attached cells were fixed, stained with Diff-Quik, and counted.

In Situ Hybridization

In situ hybridization was performed as described previously (Poulsom et al., 1998), using ^{35}S-labeled riboprobes to nephronectin (*Npnt*) (Brandenberger et al., 2001) and *Egfl6* (1548-2249 of *Egfl6* mRNA, NM_019397).

Chromatin Immunoprecipitation

Chromatin preparation and ChIP assays were performed as previously described (Donati et al., 2006) with minor modifications. Briefly, cultured primary K14ΔNβ-cateninER mouse keratinocytes (Silva-Vargas et al., 2005) were treated with 20 μM 4-OHT for 6 days and fixed with 1% formaldehyde. Crosslinked chromatin from 10^7 cells was sonicated to obtain DNA fragment sizes of about 1kb and immunoprecipitated with 8 μg of antibodies against Tcf4 (Santa Cruz, sc-8631X) or FLAG (Sigma). Q-PCR was performed with primers (Table S4) designed to amplify genomic regions of conserved putative binding sites for Lef/Tcfs. Relative sample enrichment was calculated with the following formula: $2^{(\Delta Ctx - \Delta Ctb)}$, where ΔCt x = Ct input-Ct sample and ΔCt b = Ct input-Ct control Ab.

SUPPLEMENTAL REFERENCES

Donati, G., Imbriano, C., and Mantovani, R. (2006). Dynamic recruitment of transcription factors and epigenetic changes on the ER stress response gene promoters. Nucleic Acids Res. *34*, 3116–3127.

Fujiwara, H., Kikkawa, Y., Sanzen, N., and Sekiguchi, K. (2001). Purification and characterization of human laminin-8. Laminin-8 stimulates cell adhesion and migration through alpha3beta1 and alpha6beta1 integrins. J. Biol. Chem. *276*, 17550–17558.

Poulsom, R., Longcroft, J.M., Jeffery, R.E., Rogers, L.A., and Steel, J.H. (1998). A robust method for isotopic riboprobe in situ hybridisation to localise mRNAs in routine pathology specimens. Eur. J. Histochem. *42*, 121–132.

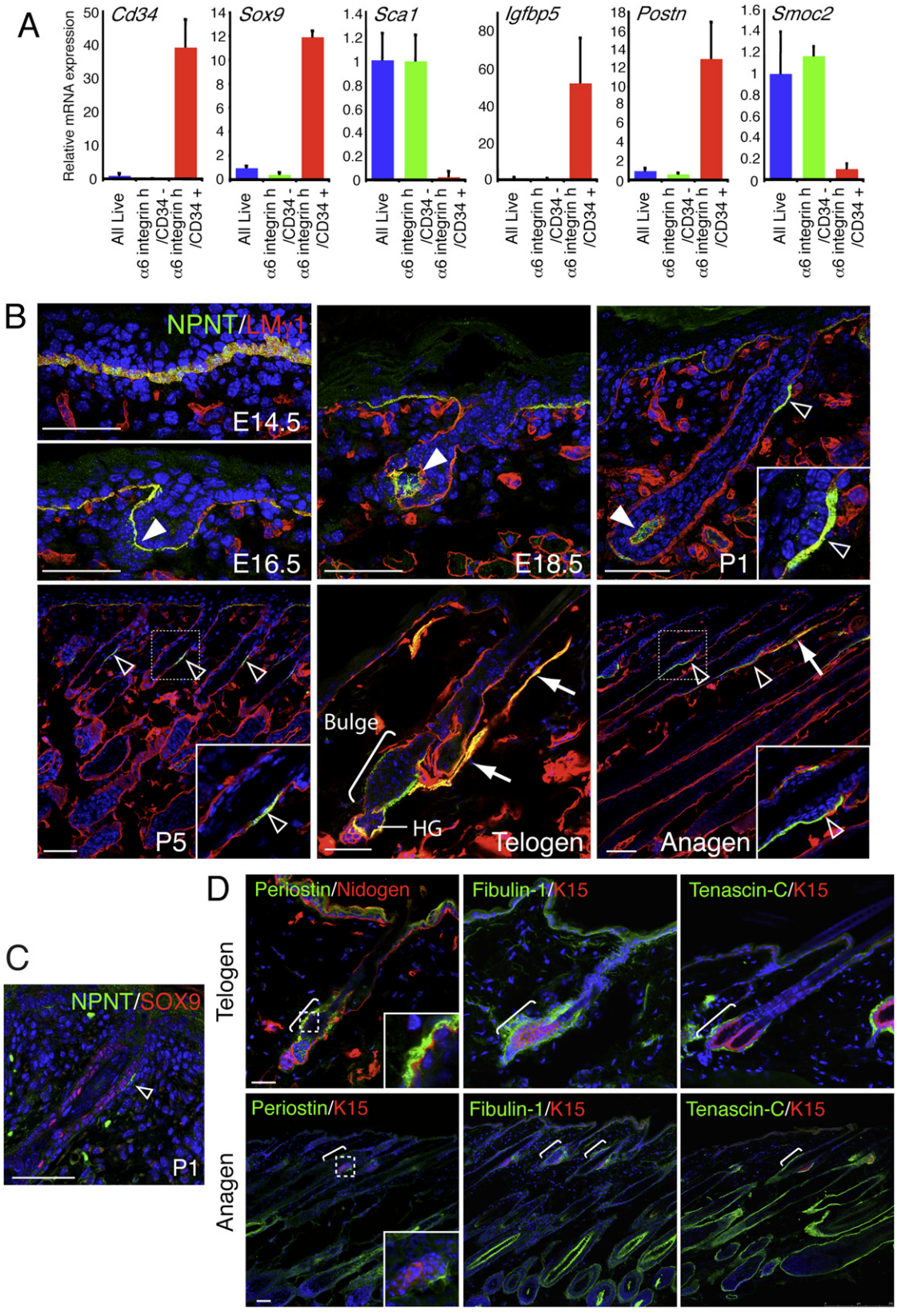
A
Relative mRNA expression
Cd34
Sox9
Sca1
Igfbp5
Postn
Smoc2
All Live
α6 integrin h
/CD34 -
α6 integrin h
/CD34 +
B
NPNT/LM-1
E14.5
E16.5
E18.5
P1
P5
Bulge
HG
Telogen
Anagen
C
NPNT/SOX9
P1
D
Periostin/Nidogen
Fibulin-1/K15
Tenascin-C/K15
Telogen
Periostin/K15
Anagen

Figure S1. Extracellular Matrix Proteins Upregulated in Bulge Stem Cells, Related to Figure 1

(A) Expression of marker genes in FACS-sorted keratinocytes was examined by Q-PCR. The bulge-specific genes *Cd34* and *Sox9* were expressed exclusively in α6 integrin^{high}/CD34+ cells, while *Sca1*, which is a marker of interfollicular epidermal progenitors, was upregulated in unfractionated basal cells (All live) and in bulge-depleted basal cells (α6 integrin^{high}/CD34 -). High expression of *Igfbp5* and *Postin* and downregulation of *Smoc2* in bulge stem cells were confirmed by Q-PCR, thereby verifying previously published microarray data. Data are means ± SEM of cells from three mice.

(B) Nephronectin deposition during skin development. Developing and adult back skin was immunostained for nephronectin (NPNT; green) and the ubiquitous basement membrane protein, laminin γ1 chain (LMγ1; red), together with DAPI nuclear counterstain (blue). Note nephronectin deposition in hair germ (white arrowheads), bulge (open arrowheads) and APM (arrows).

(C) Deposition of nephronectin in the basement membrane of Sox9-positive early bulge stem cells. A P1 back skin section was immunostained for nephronectin (green) and Sox9 (red) with DAPI counterstain (blue).

(D) Adult telogen and anagen back skin sections were immunostained with antibodies to the bulge marker K15 and to periostin, fibulin-1 (kind gift of Dr. Takako Sasaki, Shriners Hospital/Research Center, Portland, USA), tenascin-C and nidogen with DAPI counterstain (blue). Periostin and fibulin-1 were deposited around the bulge in both telogen and anagen. Tenascin-C was specifically deposited around the bulge in telogen, but was associated with the entire outer root sheath in anagen. Brackets indicate bulge. Inserts show high magnification views of boxed regions. Scale bars: 50 μm.

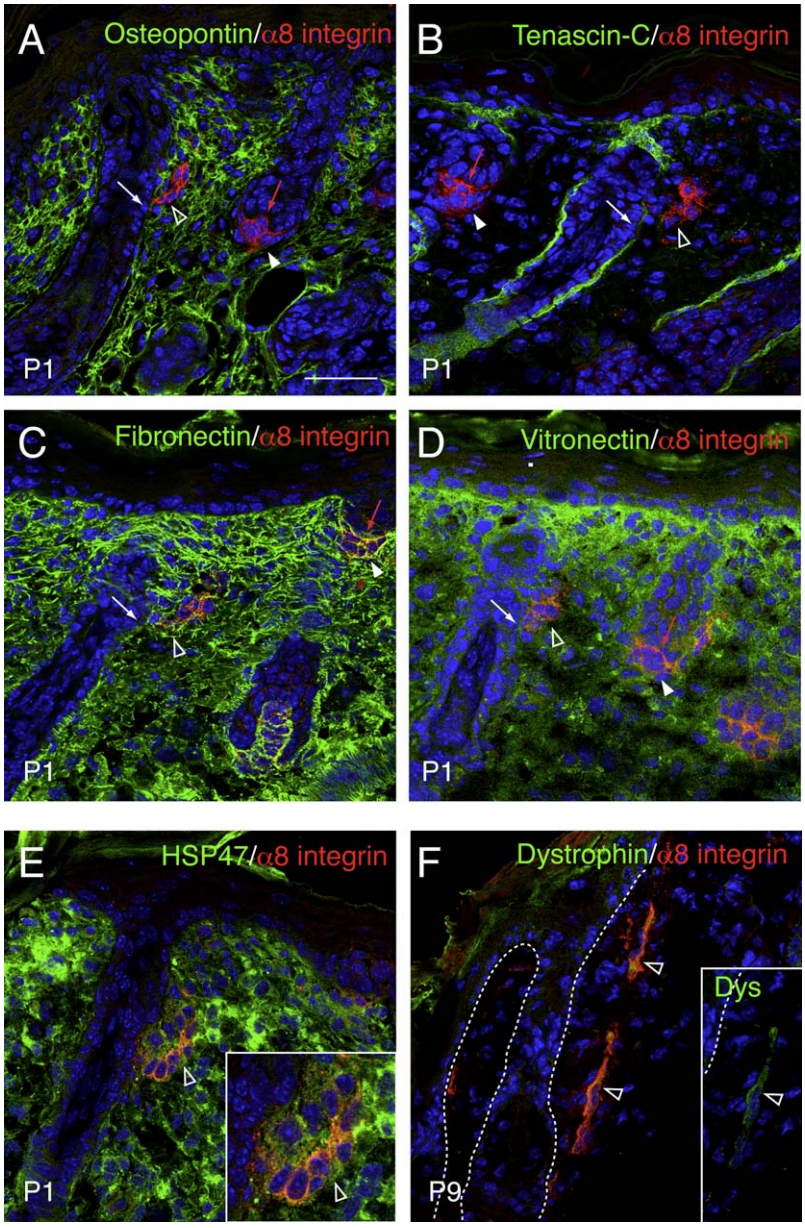

Figure S2. Distribution of α8 Integrin Ligands Other Than Nephronectin, Related to Figure 2

(A–D) Newborn P1 back skin sections were immunostained for osteopontin (A; green), tenascin-C (B; green), fibronectin (C; green), vitronectin (D; green), and α8 integrin (red), with DAPI-staining (blue). Osteopontin was deposited throughout the dermis, but not in the early bulge basement membrane (white arrow) and hair germ basement membrane (red arrow) (A) and did not colocalize with α8 integrin (A). Tenascin-C was deposited weakly in the early bulge basement membrane (white arrow) and strongly in the outer root sheath basement membrane, but did not colocalize with α8 integrin (B). Fibronectin and vitronectin were deposited throughout the dermis and showed partial colocalization with α8 integrin (D). White arrowheads indicate dermal papillae. Open arrowheads indicate α8 integrin positive-dermal cells adjacent to the early bulge. White arrows indicate basement membrane of early bulge stem cells. Red arrows indicate the basement membrane of hair germs.

(E and F) Newborn (P1 and P9) mouse back skin sections were immunostained for the dermal fibroblast marker HSP47 (green in E), muscle marker dystrophin (green in F) and α8 integrin (red), with DAPI-staining (blue). α8 integrin-positive bulge dermal cells (open arrowhead) coexpressed HSP47 (E) and dystrophin (F). Scale bar: 50 μm.

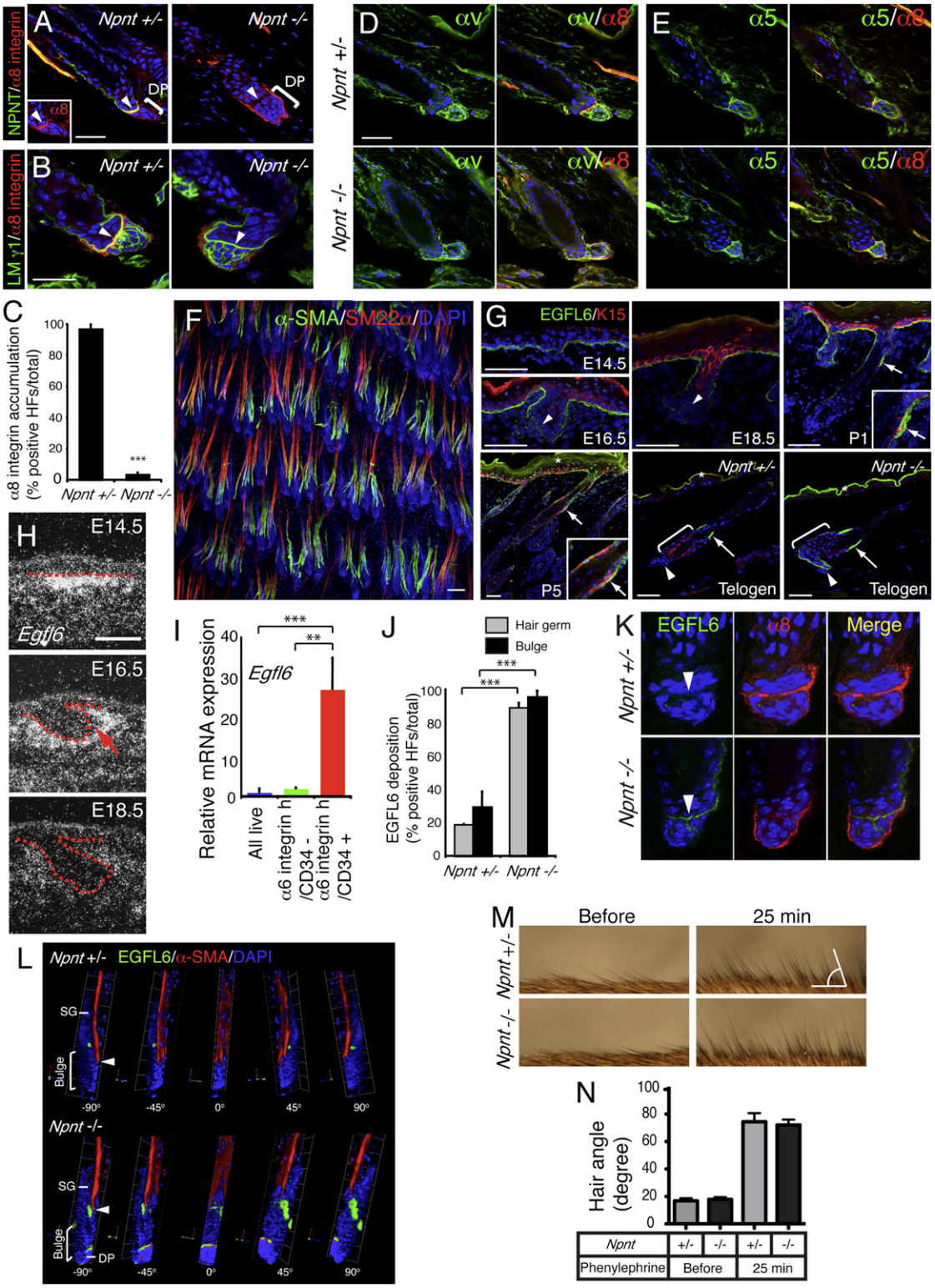

Figure S3. Analysis of Nephronectin Null Skin and Expression Pattern of EGFL6, Related to Figure 4

(A–C) Nephronectin (*Npnt*) +/− and −/− adult telogen skin sections were immunostained for nephronectin (green in A), laminin γ1 chain (green in B) and α8 integrin (red), with DAPI-staining (blue). In $Npnt^{+/-}$ control mice, α8 integrin co-localized with nephronectin at the basement membrane separating the dermal papilla and hair germ (arrowheads). However, in $Npnt^{-/-}$ skin, α8 integrin was absent from this region and was more prominently distributed at the periphery of the dermal

papilla (arrowheads). (C) Quantitation of α8 integrin accumulation at the basement membrane between hair germ and dermal papilla. Data are means ± SEM from three mice.

(D and E) Distribution of αv and α5 integrin subunits in dermal papillae of *Npnt*$^{+/-}$ and *Npnt*$^{-/-}$ skin. Sections of adult telogen dorsal skin were immunostained with antibodies against α8 integrin (red), αv integrin (green in D) and α5 integrin (green in E) with DAPI counterstain (blue). In *Npnt*$^{+/-}$ skin, αv and α5 integrins were strongly expressed in dermal papilla cells and accumulated at the basement membrane separating the hair germ and dermal papilla. In *Npnt*$^{-/-}$ skin, the distribution of αv and α5 integrins was unaffected.

(F) Wide-field maximum projection image of arrector pili muscles in back skin. Whole-mount was stained for α-SMA (green), SM22α (red), and nuclei (blue).

(G) EGFL6 (green) and Keratin 15 (red) in developing wild-type and adult telogen *Npnt*$^{+/-}$ and *Npnt*$^{-/-}$ dorsal skin. In wild-type, EGFL6 was ubiquitously deposited at the epidermal-dermal basement membrane at E14.5, but gradually disappeared from the interface between hair follicles and dermal papillae at E16.5-18.5 (arrowheads). In newborn skin (P1 and P5), EGFL6 was specifically localized in the K15-positive early bulge. In wild-type adult skin, EGFL6 showed a highly restricted localization in the basement membrane of the upper bulge (arrow). In *Npnt*$^{-/-}$ skin EGFL6 deposition in the upper bulge was increased (arrow), and EGFL6 was ectopically deposited at the basement membrane between hair germ and dermal papilla (arrowhead) (see Figure S3J). Brackets: bulge.

(H) In situ hybridization of *Egfl6*. *Egfl6* was expressed in dermal condensates at E14.5. At E16.5-18.5, *Egfl6* was expressed in dermal sheath cells, but not in dermal papillae (arrow).

(I) Strong expression of *Egfl6* in bulge stem cells. Q-PCR of mRNA from FACS-isolated epidermal cells: *Egfl6* mRNA was highly upregulated in CD34+α6^{high} bulge cells relative to other basal keratinocytes. Data are means ± SEM from three mice.

(J) Quantitation of EGFL6 deposition at the basement membrane of hair germ and bulge. In *Npnt*$^{-/-}$ skin, EGFL6 was ectopically deposited at the basement membrane of hair germ and bulge. Data are means ± SEM from three mice.

(K) Sections were immunostained for EGFL6 (green) and α8 integrin (red), with DAPI counter-stain (blue). α8 integrin did not accumulate at the basement membrane separating the hair germ and dermal papilla (arrowheads) even though EGFL6 was ectopically deposited there in the absence of nephronectin.

(L) 3D imaging of arrector pili muscles associated with single hair follicles in *Npnt*$^{+/-}$ and *Npnt*$^{-/-}$ skin. Z-stack images of dorsal skin whole mounts stained for EGFL6 (green), α-SMA (red) and nuclei (blue) were reconstructed in 3D using Volocity 5 software (PerkinElmer). In *Npnt*$^{+/-}$ skin, the arrector pili muscle attachment site is in the center of the bulge (arrowhead), which is EGFL6 negative. In *Npnt*$^{-/-}$ skin, EGFL6 was upregulated and the attachment site was in the EGFL6-positive region. DP: dermal papilla. SG: sebaceous gland.

(M and N) Induction of piloerection by injection of 100 μl of 0.2% α1-adrenergic receptor agonist phenylephrine (Sigma) in PBS into the peritoneal cavity of anesthetized *Npnt*$^{+/-}$ and *Npnt*$^{-/-}$ mice. 25min later the neck hairs (M) were photographed and the angles of guard hairs were measured with Image J software. The angles did not differ significantly between *Npnt*$^{+/-}$ and *Npnt*$^{-/-}$ mice (N). Ten hairs/mouse were measured. Data are means ± SEM from four mice. Scale bars: 50 μm, except for F (100 μm).

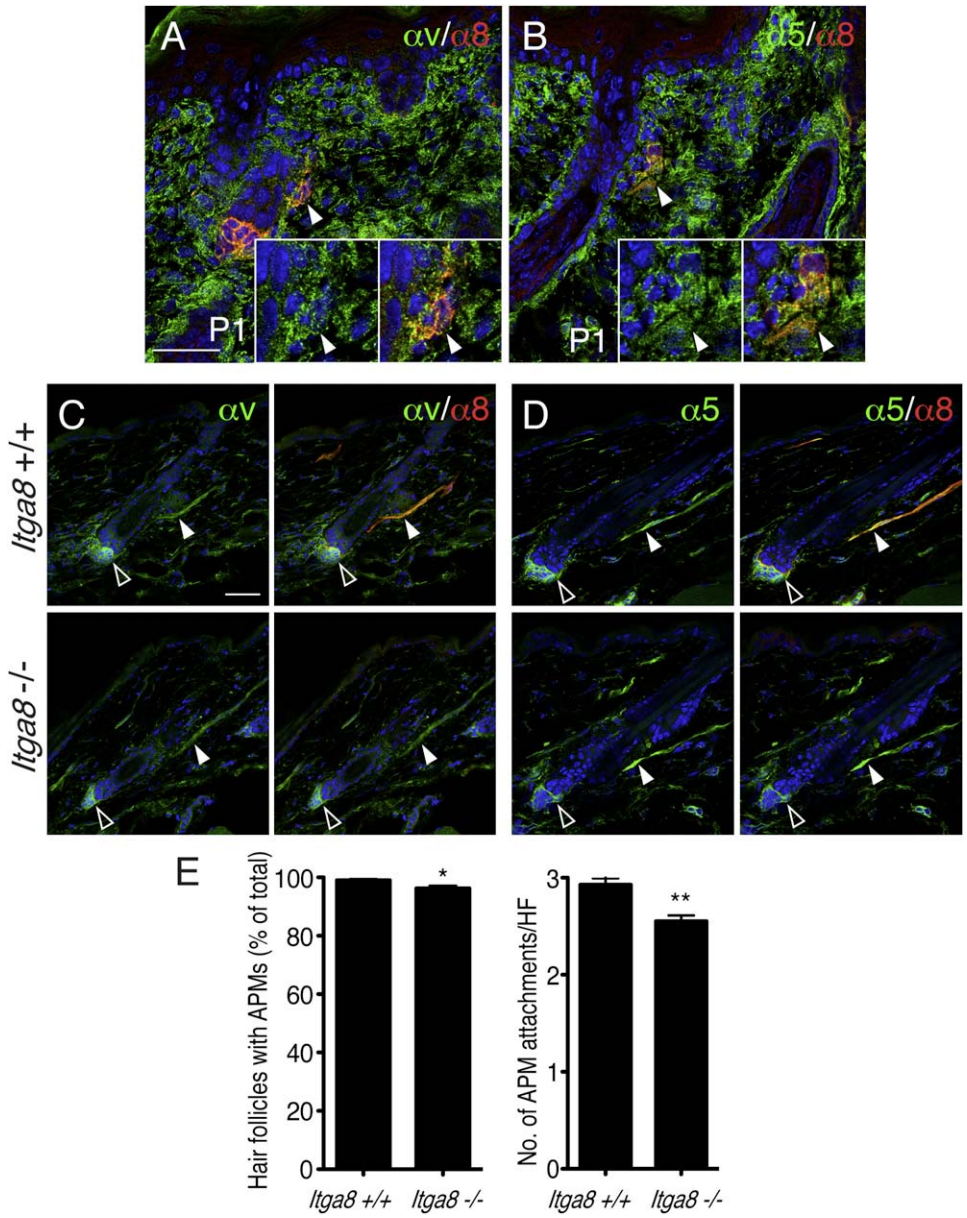

Figure S4. Expression of αv and α5 Integrin Subunits in the Arrector Pili Muscle and Reduced Arrector Pili Muscle Formation in *Itga8*$^{-/-}$ mice, Related to Figure 5

(A and B) P1 back skin sections were immunostained for αv (green in A), α5 (green in B), and α8 integrins (red), with DAPI-staining (blue). αv and α5 integrins were expressed by cells throughout the dermis, including α8 integrin-positive APM progenitors (arrowheads).

(C and D) Telogen back skin from *Itga8*$^{+/+}$ and *Itga8*$^{-/-}$ mice was immunolabeled for αv (green in C), α5 (green in D), and α8 integrins (red), with DAPI-staining (blue). αv and α5 integrins colocalized with α8 integrin in arrector pili muscles and dermal papillae of wild-type mice. In the absence of α8 integrin, αv and α5 integrins were still expressed in the APM and dermal papilla. White arrowheads: arrector pili muscles. Open arrowheads: dermal papillae. Scale bars: 50 μm.

(E) The number of follicles with arrector pili muscles and number of APM attachments per hair follicle were counted in whole-mounts of dorsal skin from *Itga8*$^{+/+}$ and *Itga8*$^{-/-}$ mice. Data are means ± SEM from four mice. A hundred follicles per mouse were examined.

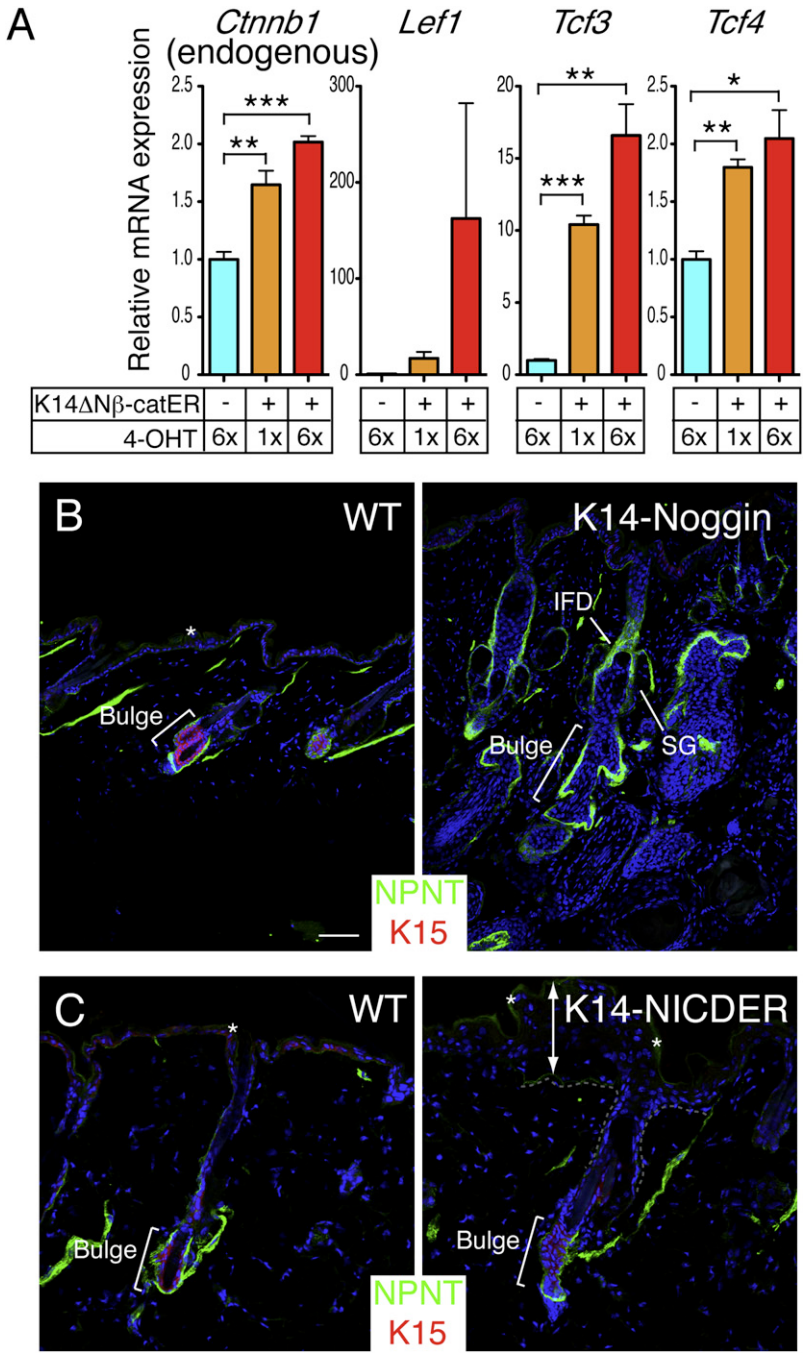

Figure S5. Regulation of Nephronectin and α8 Integrin Expression by Epidermal Wnt/β-Catenin Signaling, Related to Figure 6

(A) Upregulation of Wnt effector genes on activation of β-catenin in K14ΔNβ-cateninER skin. Epidermal expression of β-catenin *(Ctnnb1)*, *Lef1*, *Tcf3*, and *Tcf4* was quantified by Q-PCR. Adult telogen wild-type (K14ΔNβ-catER−) and K14ΔNβ-cateninER (K14ΔNβ-catER+) mice received the number of 4-OHT treatments shown. Skin was harvested and epidermis was isolated by Dispase treatment. All of the Wnt effector genes tested were upregulated upon β-catenin activation. Data are means ± SEM from three mice.

(B and C) Effects of modulating BMP and Notch signaling on nephronectin expression. (B) In K14-Noggin mice (Sharov et al., 2009) deposition of nephronectin (green) in the bulge, sebaceous gland (SG), and infundibulum (IFD) was increased. Red: K15. Blue: nucleus. (C) In 4-OHT treated K14-NICDER skin (Estrach et al., 2006) the deposition of nephronectin (green) was unaffected. Red: K15. Blue: nucleus. Asterisks: non-specific staining. Double headed arrow: thickened interfollicular epidermis. Scale bars: 50 μm.